Title: Sensory-based quantification of male colour patterns in Trinidadian guppies reveals nonparallel phenotypic evolution across an ecological transition in multivariate trait space

Running title: Non-parallel evolution of guppy colour patterns

Authors:

Lengxob Yong[1*], Darren P. Croft[2], Jolyon Troscianko[1], Indar Ramnarine[3], Alastair Wilson[1]

Affiliations:

1. Centre for Ecology and Conservation, College of Life and Environmental Sciences, University of Exeter, Treliever Road, Penryn TR10 9FE, UK

2. Centre for Research in Animal Behaviour, College of Life and Environmental Sciences, University of Exeter, Perry Road, Exeter EX4 4QG, UK

3. Department of Life Sciences, The University of The West Indies, St Augustine, Trinidad and Tobago

***Corresponding author:**

Lengxob Yong (lengxob.yong@gmail.com)

Centre for Ecology and Conservation,

University of Exeter (Penryn Campus),

Cornwall TR10 9FE,

United Kingdom

ABSTRACT

Parallel evolution, in which independent populations evolve along similar phenotypic trajectories, offers insights into the repeatability of adaptive evolution. Here, we revisit a classic example of parallelism, that of repeated evolution of brighter males in the Trinidadian guppy. In guppies, colonisation of low predation habitats is associated with emergence of 'more colourful' phenotypes since predator-induced viability selection for crypsis weakens while sexual selection by female preference for conspicuity remains strong. Our study differs from previous investigations in three respects. First, we adopt a multivariate phenotyping approach to characterise parallelism in multi-trait space. Second, we use ecologically-relevant colour traits defined by the visual systems of the two selective agents (i.e. guppy, predatory cichlid). Third, we estimate population genetic structure to test for adaptive (parallel) evolution against a model of neutral phenotypyc divergence. We find strong phenotypic differentiation that is inconsistent with a neutral model, but only limited support for the predicted pattern of greater conspicuity at low predation. Effects of predation regime on each trait were in the expected direction, but weak, largely non-significant, and explained little among-population variation. In multi-trait space, phenotypic trajectories of lineages colonising low from high predation regimes were not parallel. Our results are consistent with reduced predation risk facilitating adaptive differentiation by female choice, but suggest that this proceeds in (effectively) independent directions of multi-trait space across lineages. Pool-sequencing data also revealed SNPs showing greater differentiation than expected under neutrality and/or associations with known colour genes in other species, presenting opportunities for future genetic study.

Keywords: Parallel evolution, coloration, guppy, *Poecilia reticulata,* pool-sequencing, colour pattern analysis

INTRODUCTION

Parallel evolution is defined as the repeated, independent evolution of similar phenotypes under similar selection regimes in multiple independent populations within closely related lineages (Schluter 2004; Bolnick *et al.* 2018). Notable examples include the repeated emergence of stream and lacustrine morphotypes in sticklebacks (McKinnon *et al.* 2004; Schluter *et al.* 2004), and of thin and thick shelled habitat-specific forms of periwinkle (Butlin *et al.*, 2014). This phenomenon allows us to ask questions about the predictability of evolution. Does adaptation frequently recapitulate the same phenotypic 'solutions' to the same selective challenges? Also, what are the genetic pathways and processes involved? However, characterizing evolutionary trajectories of complex multivariate phenotypes as being either parallel or not is too simplistic. In reality, any two trajectories may be more or less aligned in phenotypic space such that the degree of parallelism lies on quantitative continuum (Stuart *et al.* 2017; Bolnick *et al.*2018). By characterizing the distribution of (multivariate) phenotypes within and among-lineages we can quantify parallelism, testing for similarity in both magnitude and direction of evolutionary trajectories over ecological transitions. We can also assess the importance of parallel (adaptive) evolution within the context of other processes contributing to phenotypic divergence (e.g. drift). Here we apply this approach to a well-known instance of putatively parallel evolution, that of replicated divergence in male colour patterns across predation regimes in the Trinidadian guppy (*Poecilia reticulata*) (Endler *et al.* 1987; Reznick *et al.* 1996).

Animal coloration and pattern traits serve many functions including signalling and crypsis (Cuthill *et al.* 2017) and have long been used to test predictions about the role of predation in driving parallel evolution (Houde, 1997; Allender *et al.* 2003; Steiner *et al.* 2009). High predation risk should select for less 'conspicuous' colours and patterns (Endler 1978, 1987; Young *et al.* 2011; Martin *et al.* 2014), but testing this may be sensitive to how colour phenotypes are quantified. Specific colour traits chosen for analysis often vary across studies even within species, while quantitative measures based on human perception (Martin *et al.* 2014) or RGB information (van Belleghem *et al.* 2018; Montenegro *et al.* 2019)

may sometimes lack ecological relevance. The latter concern arises because colour signals will (co)evolve with the visual systems (and downstream behaviours) of receiver species (i.e. the sensory drive hypothesis; Endler 1992). For instance, flower traits have coevolved with hymenopteran vision (Dyer *et al.* 2012), and variation in opsin gene sequence and expression is linked to colour polymorphism in African cichlids (Seehausen *et al.* 2008). While this means that human vision could misrepresent colour phenotypes as perceived by relevant selective agents (e.g. conspecific mates, predators), recent advances have improved our ability to model colour variation under different visual models (Stevens *et al.* 2007; Endler *et al.* 2018; Troscianko and Stevens 2015; van den Berg *et al.* 2019). Nevertheless, challenges remain such that colour and pattern phenotypes are necessarily complex and multivariate. Chromatic (e.g. colour) and achromatic (e.g. luminance) aspects of a colour signal are commonly considered, but continued reliance on univariate analyses means that the consequences of trait combinations may be overlooked (Endler and Mappes 2017). Because of these challenges, there has been a call for increased use of spatio-chromatic phenotyping approaches that integrate variation in colour with pattern (spatial arrangement) (Endler and Mielke 2005; Endler *et al.* 2018; van den Berg *et al.* 2019).

A more general limitation of many previous studies has been the relatively infrequent use of population genetic data (but see Steiner *et al.* 2009; Kratochwill *et al.* 2018). Colour traits are important targets of selective processes, but it does not follow that all divergence among populations (whether exhibiting parallelism or not) maps adaptively to local selection regime. Gene flow can sometimes preclude phenotypic divergence between populations despite differences in selection (Räsänen and Hendry 2008; Nosil 2009), while genetic drift could cause (non-adaptive) phenotypic divergence that masks parallelism (Stuart *et al.* 2017; Delisle and Bolnick 2020). Fortunately, patterns of (genome-wide) molecular genetic differentiation can be used to construct null models against which to test for and isolate the phenoptypic signal of local adaptation (e.g., Whitlock and Guillaume 2009; Pascoal *et al.* 2018a,b). There are important caveats to this however, for instance when using phenotypic variation as a proxy for quantitative genetic variation (Pujol *et al.* 2008), or when 'Isolation by

Adaptation' scenarios are plausible (e.g. Nosil *et al.* 2008; Funk *et al.* 2011). Nonethless, molecular genetic data provide an important opportunity to nuance expectations of phenotypic structuring among populations hypothesised to have undergone parallel evolution. In some cases, notably where dense marker data are available, they can also be used probe the genetic basis of phenotypic differentiation - parallel or otherwise - among populations (Elmer and Meyer 2011; Gautier *et al.* 2018).

In this study, we revisit the well-documented case of putatively parallel evolution of colour in the Trinidadian guppy by combining novel colour phenotyping methods, with estimation of phenotypic divergence among-populations in multivariate trait space and use of population genomic data. Guppies have provided important insights about many evolutionary processes (Endler 1980; Houde 1995; Reznick *et al.* 1997; Magurran 2005) with the highly variable male colour patterns receiving particular attention. Male phenotypes are subject to antagonistic sexual and viability selection; females prefer more 'conspicuous' male phenotypes but these also confer greater predation risk. In many rivers in Trinidad, upstream dispersal of piscivores, notably the pike cichlid *Crenacichla frenata*, is limited by barrier waterfalls. Downstream habitats are thus characterised by high predation risk (HP), relative to upstream low predation (LP) sites. Repeated colonization of LP sites has been associated with phenotypic shifts towards brighter, more colourful males (Endler 1983; Millar *et al.* 2006). This is presumably because the costs of being conspicuous (i.e. predation risk) are relatively lower in LP populations while the benefits (i.e. attractiveness to females) remain (Haskins *et al.* 1961; Endler 1980; Houde 1995).

We stress that these patterns of among-population variation in male guppy colour, and their interpretation with respect to predation risk have proven qualitatively robust (Millar *et al*. 2006). However, the diversity of phenotyping methods used across studies has also limited quantitative comparisons of the extent, and direction of (multivariate) evolution across lineages. Phenotyping methods have included scoring the presence/absence, number, size and position of particular colour patches (Endler, 1978; Gotanda *et al.* 2018), spectral measurements (Kemp *et al.* 2019), and spatial pattern approaches (Endler 2012; Endler *et*

147 *al.* 2018). It is also widely acknowledged that the ecological context is more nuanced than
148 described above (Endler and Houde 1995; Karim *et al.* 2007; Kemp *et al.* 2009). Predation
149 risk varies within HP and LP contexts not just between them (Endler 1995), but canopy cover
150 and light environment also differ between upstream and downstream sites, and frequency-
151 dependent selection also maintains variation within populations (Olendorf *et al.* 2006;
152 Hughes *et al.* 2013). Finally, not all predictions are fully upheld by experiments. For example,
153 low predators risk is thought to allow evolution of larger colourful spots on the body (Haskins
154 *et al.* 1961). However, in a recent study, parallel increases in melanic (black) spots occurred
155 across mesocosms lacking predators, but other colour traits changed inconsistently
156 (Gotanda *et al.* 2018).

157 Here, we assess the extent of parallel evolution in male guppy colour patterns across
158 repeated instances of LP colonisation from HP ancestors. We implement the Quantitative
159 Colour Pattern Analysis (QCPA) phenotyping approach (van den Berg *et al.* 2019) to model
160 multivariate phenotypic divergence as perceived by the two hypothesized selective agents:
161 namely the guppy (sexual selection) and the Trinidadian pike cichlid (viability selection). Our
162 specific goals are; (i) to determine whether this phenotyping approach recapitulates the
163 expected finding that LP guppies are more 'conspicuous' than HP guppies across rivers; (ii)
164 to adopt a geometric perspective (following e.g., Bolnick *et al.* 2018) to quantify the extent of
165 'parallelism' in multivariate trait space; (iii) to evaluate whether the conclusions differ with
166 respect to the two visual systems modelled; and (iv) to assess patterns of phenotypic
167 differentiation (parallel or otherwise) in the context of population genetic structure. We use
168 genomic information obtained via pool-sequencing (hereafter, Pool-seq, Schlötterer *et al.*
169 2014) to estimate genome-wide population genetic differentiation. The population genomic
170 data also allow us to (v) conduct genome wide scans with genetic regions associated with
171 phenotypic divergence, and thus conduct a preliminary investigation into the genomic basis
172 of colour patterns in the wild.
173
174

MATERIALS and METHODS

I. Sampling of wild fish

Wild guppies were sampled from 16 sites across 7 rivers in the Northern Mountain Range of Trinidad by seine nets (Table 1) in March 2017. One HP and one or two LP sites were sampled in each river except the Paria (which contributed a single LP site). Fish were transported to the University of West Indies (UWI, St Augustine, Trinidad), housed in 200L aquaria and allowed to acclimate to laboratory conditions for 5-7 days. A subset of males from each population were photographed (Table 1). Subsequently, different individuals (n ~ 100 per population) from twelve of the 16 sites were shipped live to the University of Exeter (Cornwall, UK). Although primarily for genetic investigations outwith the current study, paternal sibships produced from these wild-caught fish were used in a pilot to validate the present phenotyping strategy (see Supplemental Appendix A for details and results of validation pilot).

II. Phenotyping of male colour traits

Visible and UV-spectrum photography (Figure 1) were carried out using a Samsung NX1000 camera converted to full spectrum, fitted with a Nikkor EL 80mm lens out on live, unsedated fish housed in a custom designed UV-transparent water filled chamber, as detailed in Appendix A. After photography, fish were humanely euthanized in a lethal dose of buffered MS-222 and tissue preserved in RNAlater (Invitrogen). Photographs were analysed using the QCPA framework, which quantifies colour traits using images and species-specific visual system parameters (see www.empiricalimaging.com and van den Berg *et al.* 2019). In addition to chromatic and achromatic signals, QCPA allows incorporation of spatial information using the geometric arrangement colour patches (with discrimination of adjacent patches based on the receptor noise estimate ΔS; Vorobyev and Osorio 1998). This has ecological relevance because, in behavioral trials, female guppies prefer males that are more conspicuous in colour pattern or have higher discriminant values (Sibeaux *et al.* 2019). We quantified colour variation over the whole body (excluding head, tail and fins), using four

complementary traits: saturation boundary strength $sat_{\Delta S}$, luminance boundary strength $lum_{\Delta S}$, chromaticity boundary strength $chrom_{\Delta S}$ and chromaticity boundary strength variation $CoV_{\Delta S}$ (Endler *et al.* 2018). Together, these measures represent the chromatic (saturation and hue), achromatic (luminance), and spatial (size and position of colour pattern elements) properties of colour patterns. Simplistically, the first three of these can be thought of as describing the "grayness" difference, "brightness" difference, and colour contrast between neighbouring patches respectively. Higher values indicate higher internal contrasts across colour-patch boundaries and/or more boundaries. The final metric describes the variation in colour contrast between patches (i.e. it would be higher if there are both high-contrast *and* low contrast internal boundaries). We used whole body trait measures for two reasons. First, specific pattern elements (i.e. colour patches at particular body locations) differ greatly within and among-populations. Thus, designating universally comparable phenotypes from discrete pattern elements is problematic. Second, female guppies likely select males based on groups of colour patches not single elements (Cole and Endler 2015).

For each photograph, the four traits were scored under two visual system parameter sets; a conspecific (guppy) vision model and a predator (pike cichlid, *Crenacichla frenata*) vision model. Note that *Crenacichla* is used because it is widely viewed as the most important selective visual predator in guppies, although it is not present at the high predation sites sampled in the Yarra and Marianne in this study. The parameters sets included user specified values of (i) receiver spectral sensitivities (the relative abundance of their cones and rods in the retina), (ii) receiver visual acuity, and (iii) physical distance at which the receiver might be from a male guppy. The use of two visual systems reflects our view that perception of male coloration may well differ between receiver species imposing selection (i.e. a pattern that is more conspicuous to a female guppy may not always be so to a cichlid predator).

Support for this possibility was provided by a pilot validation study used to check the suitability of phenotyping methods for detecting genetic variation in male colour and pattern (see Appendix A for full methods and results). Briefly photographs of males from known

paternal sibships produced using wild caught parents were processed using our QCPA pipeline. Data analysis confirmed moderate to high sire level repeatabilities (analogous to heritabilities) for all traits under both visual models as expected (since male colour is partly Y-linked; Lindholm and Breden, 2002). This confirms the QCPA approach effectively characterises genetically meaningful phenotypic variation. Importantly, (paternal) family correlations (r_F) between homologous traits defined under alternative vision models (e.g., *chrom*$_{\square S}$ based on guppy and cichlid vision models) are positive, but also significantly less than +1 in three of four cases. Using r_F as an estimate of the additive genetic correlation (Astles et al. 2006), this indicates homologous metrics defined under the two vision models are genetically distinct (if correlated) traits.

III. Generation of Pool-Seq data

To test characterise population genetic structuring we used a Pool-seq approach to obtain allele frequency estimates (Gautier *et al*. 2013; Schlötterer *et al.* 2014). While this approach is cost effective, available funding and tissue samples limited inclusion to 12 of the 16 wild populations (with guppies from the Turure (TH and TL) and Guanapo (GL1 and GL2) rivers excluded). With these exceptions, genomic DNA samples were obtained for 40 fish (20 males; 20 females) per population, using a Qiagen DNAeasy kit (Qiagen Co). For each sample, the concentration and purity of the genomic DNA were measured and using a Nanodrop spectrophotometer and q-bit (Thermo Fisher Scientific). Purity was further checked on a 1% agarose gel before sex-specific DNA pools were created for each population (n = 24; 12 populations by 2 sexes). Pools, each containing equal DNA concentration from 20 individual fish, were sequenced at the Earlham Institute (Norwich, UK). Barcoded DNA paired end libraries with insert size of approximately 150bp were prepared using Illumina Truseq HT library prep and sequenced on 2 lanes using Illumina NovaSeq (Illumina Inc., California, USA). Raw paired-end reads were checked for quality using FastQC, and adapters were verified and removed using *cutadapt*. To investigate among population differences, the raw reads of male and female pools for each population

were merged. Reads were then mapped to the reference guppy genome (Guppy_female_1.0+MT, GCA_000633615.2, Künster *et al.* 2016) with BWA mem (Li and Durbin 2010) using default parameters to generate initial BAM files. Aligned reads were then sorted, marked for duplicates and indexed, to generate final BAM files using Samtools v1.9 (Li *et al.* 2009). All BAM files were merged to create a mpileup file (i.e. samtools mpileup –f), which was subsequently filtered for indels and then used to generate a sync file (mpileup2sync.jar; base quality > 20 or --min-qual 20) containing allelic frequency information for every population using *Popoolation2* (v1.201) (Kofler *et al.* 2011). A clean sync file was then obtained after indel removal (filter-sync-by-gtf.pl), and subsequently used for downstream population genomic analyses.

IV. Data analysis

The phenotypic data set comprised measures of 8 response variables (sat_S, lum_S, $chrom_S$, CoV_S x 2 visual system models) for 388 male guppies representing 16 distinct populations (6 HP and 10 LP) from 7 rivers. The genomic data comprised of 24 pools of DNA-seq data (12 populations x 2 sexes), whose summary statistics are described in the Supplemental (Table S1). In brief, each pool generated between 362-599M reads with a mean Phred score of 35.8 and 96x depth of coverage. Between 88-98% of raw reads were successfully mapped to the guppy female reference genome assembly. Unless otherwise stated, all statistical analysis was done in R (R Core Team 2019) with ASReml-R (Butler *et al.* 2017) used to fit mixed models. Full R codes and citations to all packages, bash scripts, and Javascripts for colour analysis will be provided in the supplemental materials upon publication.

Testing effects of population and predation regime

We first plotted trait means (by river and overall), to check whether differences between populations and or predation regimes (HP versus LP) were visually apparent. We then fitted univariate mixed models to each trait, including a random effect of *population* (i.e. sampling

site) and a fixed effect of predation *regime* (as a two level factor). This allowed us to estimate variance among *populations* (V_{Pop}) conditional on the fixed effect of *regime* (i.e. as the among-population variance not explained by *regime*). We scaled traits to standard deviation units before analysis such that V_{Pop} can be interpreted as an intra-class correlation unadjusted for fixed effects. We also estimated the adjusted population level repeatability (R_{Pop}) for each trait (i.e., V_{Pop} as a proportion of total variance conditional on the fixed effect). Statistical inference on the fixed effect was by Wald F tests and we used likelihood ratio tests (LRT) to assess the significance of the random effect. For the latter, we assumed that twice the difference in log-likelihoods between full and reduced (with no random population effect) is distributed as a 50:50 mix of χ^2_0 and χ^2_1 (subsequently denoted $\chi^2_{0,1}$; Stram and Lee 1994).

Multivariate models and estimation of pairwise phenotypic distance

We built a multivariate mixed model of all 8 traits. A random effect of population was included on each trait but with no fixed effects (except intercepts). This yielded an estimate of the among-population variance-covariance matrix (**D**), containing among-population trait variances (but no longer conditional on any *regime* effects) on the diagonal, as well as covariances that were scaled to among-population correlations (r_{Pop}) between all trait pairs. We assume approximate 95% CI of r_{Pop}±1.96 SE.

We then used the fitted multivariate model to predict pairwise phenotypic distances between multivariate population means by extracting the best linear unbiased predictions (BLUP) of trait means by population and calculated the 16x16 (since $n_{population}$=16) Euclidean distance matrix (**E**) among populations in n_{trait}-dimensional trait space. We used all 8 traits ($\mathbf{E}_{all}$), but also generated the matrices based on guppy ($\mathbf{E}_{gvm}$) and cichlid ($\mathbf{E}_{cvm}$) vision model traits respectively. Note that uncertainty in BLUP is not reflected in the point estimates of $\mathbf{E}_{all}$, $\mathbf{E}_{gvm}$ and $\mathbf{E}_{cvm}$, but we use these matrices to visualise patterns of among-population divergence not as a basis for robust statistical inference. Specifically, neighbour-joining trees based on $\mathbf{E}_{all}$, $\mathbf{E}_{gvm}$ and $\mathbf{E}_{cvm}$ were plotted to assess any tendency to cluster by *regime*. For

each population pair, we also plotted the distance based on the guppy vision model against the corresponding cichlid distance to assess whether (i) a relationship between $\mathbf{E}_{gvm}$ and $\mathbf{E}_{cvm}$ is apparent, and ii) phenotypic distances tend to be lower for within- versus across-*regime* population pairs.

Testing for association of phenotypic and genetic distance

For the subset of 12 populations with molecular as well as phenotypic data, we used the sync file to estimate genome-wide differentiation among populations using the fixation index (F_{ST}). F_{ST} was calculated for single nucleotide polymorphisms (SNPs) in 50k windows using *fst.sliding.pl* implemented in *Popoolation2* (parameters: –min-count 2 –min-coverage 4 –max-coverage 80 –pool-size 80 –window-size 50000 –step-size 50000), which calculates F_{ST} following Hartl and Clark (1997). The resultant among-population F_{ST} matrix was compared to phenotypic distance estimates in two ways. First, we used Mantel tests to assess the correlation with phenotypic distance (represented by $\mathbf{E}_{all}$, $\mathbf{E}_{gvm}$ and $\mathbf{E}_{cvm}$ sub-setted to the 12 populations with SNP data). Second, following Pascoal *et al.* (2017) we refitted univariate mixed models to each of the 8 response variables, but this time with no fixed effects and a modified random effect structure to total V_{Pop} (i.e. not conditional on *regime*) into two components: one attributable to divergence under neutral processes (i.e. drift; $V_{Pop.N}$); and another attributable, under some assumptions, to divergence under selection (from predation, sexual selection and/or unknown selective agents; $V_{Pop.S}$).

This second approach, follows the same premise as Q_{ST}-F_{ST} comparisons (Leinonen *et al.* 2013), and asks whether there is more quantitative phenotypic divergence among-populations than expected from levels of (putatively) neutral molecular divergence. To implement it, we ran models with two random effects of population identity, one which covaries among populations according to their molecular 'relatedness' structure, and a second which is uncorrelated across populations. For the former we assume phenotypic covariance between fish sampled from populations *i* and *j* that is attributable to neutral population effects is equal to $S_{ij} \cdot V_{Pop.N}$ where S_{ij} is genome-wide 'similarity' between the

343 populations. Since F_{ST} inscreases wih dissimilarity we define $S_{ij} = 1 - {F_{ST_{i,j}}}/{F_{ST_{max}}}$ where

344 $F_{ST_{max}}$ is the highest observed pairwise F_{ST} among the populations sampled. This simply

345 scales S_{ij} from a maximum of 1 (when i=j) to 0 (for the most differentiated pair of

346 populations). To test whether trait variation among populations is greater than expected

347 under neutral divergence alone, we compared the model with both variances to one where

348 $V_{Pop.S}$ is absent using LRT. Two caveats to this method shoud be noted: first, it assumes that

349 to a first approximation genome-wide F_{ST} measures neutral differentiation (i.e. from drift and

350 gene flow); second, since we are modelling phenotypic variation in wild caught fish rather

351 than in a common-garden experiment, any contributions to population divergence from

352 phenotypic plasticity are likely to be partitioned into $V_{Pop.S}$ (Pujol *et al.* 2008).

353

354 *Multivariate models for estimating parallelism among replicate population pairs*

355 Phenotypic analyses described above are 'blind' to the ancestral versus derived

356 status of HP and LP population pairs with rivers. Therefore, we also adopted recent

357 methods that use phenotypic change within lineages to quantify parallelism (De Lisle and

358 Bolnick 2020). We assume that within each river, an HP and LP pair can be viewed as

359 representing a 'lineage' in which the HP is ancestral. This assumption yielded 9 'lineages'

360 among the 16 populations with phenotypic data. Fish from the Paria are excluded as there is

361 no HP site, but the Aripo, Guanapo, and Marianne rivers each contribute two 'lineages' (i.e.

362 HP-LP comparisons). We describe the approach briefly, using notion from De Lisle and

363 Bolnick (2020) and referencing their equation numbers. First we calculated, the n_{trait} row by

364 $m_{lineage}$ column data matrix **X**, where each element of **X** represents $\Delta z_{n,m}$ (the difference in

365 mean standardized phenotype (z) between HP and LP populations for trait n in lineage m;

366 Equation 3). Each row of **X** thus represents the vector of phenotypic change from HP to LP

367 within a lineage in multi-trait space. **X** was used to calculate **C**, the (m x m) among-lineage

368 correlation matrix of phenotypic change vectors which was then subject to eigen

369 decomposition (following Equations 5 and 6). To mirror our investigation of the among-

population distance matrices (i.e. $\mathbf{E}_{all}$, $\mathbf{E}_{gvm}$ and $\mathbf{E}_{cvm}$), we calculated and decomposed **C** matrices based on $sat_{\square S}$, $lum_{\square S}$, $chrom_{\square S}$ and $CoV_{\square S}$ determined using both vision models ($\mathbf{C}_{all}$), but also using guppy ($\mathbf{C}_{gvm}$) and cichlid vision model ($\mathbf{C}_{cvm}$) traits, separately.

In the case that multivariate trajectories are perfectly parallel across all lineages, the first eigen vector of **C** should explain all variation and all lineages would load on this vector with the same sign (but differing magnitudes if the extent, rather than direction, of phenotypic change differed among lineages). In contrast, a uniform distribution of eigen values (meaning low among-lineage correlations of change vectors), and/or a mixture of positive and negative lineage-specific loadings on the first eigen vector is expected under non-parallelism. As suggested by De Lisle and Bolnick (2020), for the case of fewer traits (here 4 or 8 depending on the version of **C**) than lineages (here 9), we generated a null distribution of *m* eigenvalues by simulating 1000 random vectors representing evolutionary change under independence (among lineages) of multivariate phenotypic trajectories. While acknowledging that power to reject the null (no parallelism) may be low (De Lisle and Bolnick 2020), observed eigenvalues were then compared to the simulated distribution. An eigenvalue of **C** greater than 95% of values simulated assuming independence is taken as statistical support for parallelism.

Genotype-phenotype association mapping from pool-seq data

Leveraging the pool-seq data, we tested for relationships between allele frequencies at SNP loci and phenotypic variation (colour metrics: $sat_{\square S}$, $lum_{\square S}$, $chrom_{\square S}$ and $CoV_{\square S}$) and predation regime (*high* vs *low*). We did this using genome-wide scans for association in BayPass (Gautier, 2015). This method identifies loci more with higher than expected differentiation among populations based on the *XtX* statistic (Gunther and Coop 2013), and alsotests associations between SNPs and population-specific covariables (while accounting for background population structure from drift and gene flow). Since direct selection on male coloration is necessarily sex-limited, we elected to use SNP data from male pools only for these analyses (rather than combined male and female data used for genome wide F_{ST}

398 estimates). Major and minor allele counts for each SNP were calculated for each population
399 from the previously compiled sync file using the *snp-frequency-diff.pl* script with the following
400 parameters (–min-coverage 75 –max-coverage 200). Using custom awk scripts, allele
401 counts were extracted and formatted for BayPass's input genotype file (Gautier 2015). The
402 large number of calculated SNPs from the male pools (ca. 5,977,803 SNPs) mainly on
403 known linkage groups (LGs) were then subsampled to yield about 100k SNPs along the
404 whole genome (Mean = 95,911 ± 61.2 SNPs from known LGs only, corresponding to about
405 4170 per LG) to generate about 100 sub-datasets. Subsets were then analysed individually
406 using the BayPass core and standard covariate models. The resulting population covariance
407 matrices of allele frequencies (interpretable as similarity matrices) were generated under the
408 core model and checked for consistency across all data subsets by calculating the distance
409 among matrices (hereafter FMD) using the *fmd.dist* function (Figure S1; Table S2). The
410 mean FMD among all pair wise comparison was 0.2 (with $r > 0.99$ for all pairwise
411 comparisons).

412 To identify SNPs that deviated from neutral expectations we used *simulate.baypass*.
413 This uses the population covariance matrix to simulated 'pseudo-observed datasets' (POD),
414 assuming SNP neutrality, consistent with the demographic history. This allows a null
415 distribution of the *XtX* to be generated, the 99% quantile of which was used as a significance
416 threshold (median $XtX > 21.2$) to determine whether observed SNPs were under selection.
417 We then used the BayPass IS covariate models, and resultant Bayes Factor (BF) to test for
418 association between SNPs and population level male colour traits (and/or predation regime)
419 (Gunther and Coop 2013; Gautier 2015). Evidence for significant association between SNP
420 and a tested covariate was based on BF > 30db (Gautier 2015).

421 Finally, we checked whether SNPs identified as deviating from neutrality and/or
422 associated with a covariate showed enrichment for gene ontology (GO) categories and
423 functions. We extracted the corresponding identity of genes or nearby genes, which and
424 blasting against the zebrafish genome (*Danio rerio* NCBI Refseq GCF_000002035.6, Howe
425 *et al.* 2013) for annotated orthologs. The annotated orthologs were run in the gene ontology

resource (http://geneontology.org/, Ashburner *et al.* 2000; The Gene Ontology Consortium 2019).

RESULTS

I. Non-significant predation regime effect on and among-population variance in male colour patterns

Mean values of $chrom_{\Delta S}$, $cov_{\Delta S}$, $sat_{\Delta S}$ and $lum_{\Delta S}$ varied considerable between vision models and populations (Figure 2a-d). Qualitatively, the guppy vision model detected less variability among populations and tended to yield higher (more conspicuous) values for $chrom_{\Delta S}$ and $sat_{\Delta S}$ relative to cichlid vision (with the converse for $cov_{\Delta S}$ and $lum_{\Delta S}$). Differences between HP and LP regime were not consistent across traits and rivers, although overall (i.e. across rivers) trait means were higher in LP guppies for all 8 traits.

Univariate mixed models confirmed this pattern, but provided limited statistical support for differences in trait means between HP and LP (Table 2). Positive *regime* coeffcients for all traits indicated a tendency to higher conspicuousness at LP sites; but across the eight models, only $lum_{\Delta S}$ under the guppy vision model was significant (coefficient (SE): 0.83 (0.37) sdu, $P < 0.03$; Table 2). A moderately large yet non-significant effect (+0.57 sdu) was estimated for $chrom_{\Delta S}$ under the cichlid model, while the average estimated *regime* effect size of *regime* +0.328 sdu. Support for strong among-population differentiation, over and above any *regime* effects was unequivocal; LRT comparisons to reduced models with no population effect yielding $P<0.001$ for all traits (Table 2). Population level (conditional) repeatability R_{Pop} ranged from 30% to 71% with an average of 54%. R_{Pop} estimates were very close to V_{Pop} indicating that *regime* explained little of the among-population differentiation (if *regime* explained large amounts of trait variance, then in these models $V_{Pop} + V_R$ would <1 leading to a systematic finding of $R_{Pop}>V_{Pop}$).

II. No clustering of guppy colour patterns by predation regime

The **D** matrix (estimated without conditioning on *regime*) yielded V_{Pop} estimates very similar to (conditional) estimates obtained from univariate models (Table 3). The correlation structure within **D** was not universally positive (which is the expectation if populations varied along a simple axis from greater to less conspicuousness; Table S3). Population-level correlations between homologous traits defined using guppy and cichlid vision models were positive but significantly less than +1 (assuming an upper 95% confidence interval of r_{Pop} + 1.96 SE). Specifically r_{pop} (SE) were estimated as 0.65 (0.16), 0.39 (0.23), 0.28 (0.24) and 0.09 (0.28) across the two models for $sat_{\Delta S}$, $lum_{\Delta S}$, $chrom_{\Delta S}$, and $CoV_{\Delta S}$ respectively.

Phenotypic distance matrices derived from the multivariate mixed model fit provided little support for clustering of populations by *regime* in multi-trait space (Figure 3, Table S4). Using distance defined from all traits at once and guppy vision models, there was arguably some patterning (e.g., upper right portion of Fig 3a contains a grouping of 6 LP populations with 1 HP whereas Fig 3b has a grouping of 6 LP and no HP), but this is less apparent using just the traits subsets from the predator or cichlid (Figure 3c) vision model.

Pairwise phenotypic distances (using either guppy vision or cichlid vision traits) did not suggest shorter average pairwise distances between populations within- versus across-predation regimes (Figure 4). If clustering by *regime* was present, we would expect higher phenotypic distances for low-high predation (LH) comparisons than for low-low predation (LL) or high-high predation (HH) (i.e. the ellipse of red LH points in Figure 4 would be shifted to higher values on x and/or y axes than the blue ones; Figure 4). Two further points emerge from Figure 4; first, there is no apparent relationship between the pairwise population distance estimates defined by the two vision models. Population pairs that are more distinct with respect to guppy vision are not generally more distinct under the cichlid vision model. This is consistent with the absence of strong positive r_{POP} between homologous traits noted above. Second, the 95% confidence ellipse of pairwise distances for HH comparisons is smaller and shifted to lower values (on both axes) relative to HL or LL comparison. This

pattern implies that there may be lower phenotypic variance among high predation populations that among low predation populations. To investigate further, we fitted post hoc multivariate mixed models (described Table S5) to regime specific data subsets, and compared total phenotypic variance among-populations (calculated as the trace of regime specific **D** matrices). Point estimates corroborated our interpretation of Figure 4, the trace of $\mathbf{D_H}$ being 65% of the trace of $\mathbf{D_L}$. However, unsurprisingly given the number of populations in each regime, our trace estimates were characterized by high uncertainty and the difference is not statistically significant.

III. Phenotypic differentiation does not align with putative neutral genetic divergence

Consistent with previous studies (e.g., Suk and Neff 2009; Willing *et al*. 2010; Fraser *et al.* 2015), genome-wide pairwise F_{ST} comparisons revealed strong genetic structuring by river and drainage (Figure 5; Table S6). There was almost no correlation between molecular differentiation and estimated phenotypic distance (Mantel test of F_{ST} matrix correlation with $\mathbf{E}_{all}$ r=-0.049, P=0.608; with $\mathbf{E}_{gvm}$ r=0.026, P=0.426; and with $\mathbf{E}_{cvm}$ r=-0.033, P=0.569). A neutral model of among population divergence was also rejected (at α=0.05) for 6 out of 8 traits using our mixed model strategy to partition V_{Pop} into components attributable to neutral ($V_{Pop.N}$) and selective ($V_{Pop.S}$) components (Table 3). The proportion of trait variance explained by the latter was considerably higher than by the former for most traits. Under the cichlid vision model, $sat_{\Delta S}$ and $chrom_{\Delta S}$ proved exceptions to this pattern, with the more complex model offering no improvement to model fit and $V_{Pop.S}$ being bound to zero. Thus, with these two exceptions, genome wide-molecular divergence among populations cannot readily explain the phenotypic differentiation structure.

IV. Non-parallelism in guppy colour pattern among lineages

Decompositions of the three **C** matrices revealed a highly skewed distribution of eigenvalues (Table 4). However, since the rank of **C** is limited to the smaller of n (traits, here either 4 or 8) and m (lineages, here 9) all three 9 x 9 **C** matrices will necessarily be rank

509 deficient. In this context, eigen values of zero are inevitable and not biologically informative.
510 Moreover, the first eigenvectors were not particularly dominant, capturing 55%, 51% and
511 40% of $\mathbf{C}_{gvm}$, $\mathbf{C}_{cvm}$ and $\mathbf{C}_{all}$ respectively, while lineages loaded on this first eigenvector with a
512 mixture of positive and negative signs. The structure of the **C** matrices was thus not
513 consistent with parallel phenotypic evolution among these lineages in 8-trait space, or in
514 either of the 4-trait spaces. Random vectors provided no evidence that the first eigen values
515 were larger than expected under a null model of independent evolutionary trajectories across
516 lineages (Figure S2). The second eigen values of $\mathbf{C}_{gvm}$ and $\mathbf{C}_{all}$ were greater than 95% of
517 simulated values, which suggested some overdispersion and thus deviation from complete
518 independence. However, lineages also loaded on this second eigenvector with a mix of
519 signs too (in all three **C** matrices) so we cannot interpret this as parallel evolution in a
520 direction defined by the second axis of **C**. We suspect that this signal of non-independence
521 arises because data from single high predation populations in Aripo, Guanapo, and
522 Marianne rivers each contributed to the vectors of phenotypic change for two lineages (i.e.
523 HP vs LP comparisons within-river).
524
525 **V. Genome-phenotype association analysis reveals that differentiated SNPs are found**
526 **in genes related to cell morphogenesis and neural development.**
527 The core BayPass model revealed 85 SNPs more differentiated among populations
528 than expected under neutrality at the 0.01% POD significance threshold (Figure 6). Of these,
529 61 and 24 were located within genic and non-genic regions, respectively (summarized in
530 Table 5). Some of the genes were orthologous to zebrafish genes documented to be
531 involved in cell morphogenesis and cell projections, colour patterning and pigmentation (e.g.
532 *xpc, rpl, rilp, netrins*). Some were also within genes involved in neural development, such as
533 sensory axon guidance (e.g. *ptprfa*). Using orthologous zebrafish genes determined by
534 blasting, our GO analysis found no enrichment for any gene ontology category.
535 Using the BayPass IS model, we found a total of 195 SNPs associated with a tested
536 covariate using a BF threshold > 30db (colour traits: guppy vision model = 77; cichlid vision

model = 101; predation = 17, summarized in Table S7). Interestingly, there was no overlap with the 85 differentiated SNPs identified under the core model. Taken at face value, this suggests SNPs identified by the core model as being more differentiated than expected are not related to colour pattern differences among populations. SNPs significantly associated with covariates in the IS model were scattered throughout the genome (not clustered on specific chromosomes), and found within both non-genic and genic regions (~42% in non-genic regions). With a single exception (LG22: 9903588; associated with both measures of $sat_{\Delta S}$) SNP-colour trait associations differed between between the guppy and cichlid visual perceptual models, consistent with the finding that traits defined under the two models have different genetic underpinnings. As with the *XtX*-based results from the core model, many SNPs associated with covariates under the IS model were found in genes previously implicated with cell morphogenesis and neuronal functions (e.g., *hapln2*; Table S7). There was no enrichment of genes related to any functional processes using putative genes identified from SNPs associated with traits under the guppy visual model. However, we found enrichment of genes for nervous system development, anatomical structure morphogenesis, and cellular process using SNPs associated with the traits defined usng the cichlid visual model ($P < 0.0001$, Table S8). Interestingly, some of the non-genic SNPs with elevated BF values were near genes that have known roles in teleost patterning (e.g. *bnc2, cdh11,* for full list see Table S9 and S10).

DISCUSSION

Using colour traits defined by the visual systems of two major agents of selection on colour in male guppies (conspecifics, cichlid predator), we found an overall tendency towards higher, more conspicuous, phenotypic means in LP guppies as predicted. However, (i) trait means are not systematically higher at LP for within-river comparisons, (ii) statistical support for predation regime effects are weak, and (iii) regime effects explain little of the total among-population differentiation. Moreover, when modelling colour variation in multivariate phenotypic space we find (iv) little support for clustering of populations by predation regime,

565 and (v) no evidence for parallel evolution of lineages. Nevertheless, putatively neutral
566 patterns of genome-wide molecular differentiation did not readily explain the among-
567 population phenotypic structure. This suggests that adaptive evolutionary processes have
568 caused divergence of male colour among populations. Here, we first discuss these
569 phenotypic patterns and their interpretation in relation to the evidence for parallel evolution of
570 brighter male colouration across the high to low predation ecological transition in guppies.
571 We then comment on the results of our genomic analyses that revealed some SNPs
572 differentiated among populations in (or close) genes implicated in pigmentation, patterning
573 and neuronal development in other fish species.
574
575 **Patterns of among-population phenotypic differentiation**
576 Traits derived from the novel QCPA phenotyping pipeline offer only qualified support for the
577 longstanding view that guppies from LP populations are particularly colourful and
578 conspicuous (Haskins 1961; Endler 1980; Millar *et al.* 2006). Thus, trait means are higher at
579 LP overall, but this is not a statistically robust pattern. Nor is it found consistently across the
580 HP to LP transition within rivers. The lack of stronger patterns is perhaps somewhat
581 surprising, although we note that previous guppy studies have also reported similarly
582 inconsistent differences across regimes within rivers using transplant (Dick *et al.* 2018;
583 Kemp *et al.* 2009, 2018) and predator-manipulation experiments (Gotanda *et al.* 2018).
584 Colour differentiation between populations is strong using the QCPA phenotyping approach
585 (approximately half of all phenotypic variance is among-populations), but predation regime
586 does not explain much among-population variance (in single traits or multivariate
587 phenotype). This conclusion is further supported by the finding that populations do not
588 obviously cluster by predation regime in multi-trait space, regardless of whether this space is
589 defined in 8 dimensions (using all traits defined from guppy and cichlid visual models) or 4
590 (i.e. using just guppy or just cichlid perception). Nor does correlation structure in the
591 population variance-covariance matrix (**D)** supports the presence of a single major axis of
592 variation running from low (i.e. low trait values) to high conspicuity.

In principle these results could occur even with parallel evolution of replicate lineages across the HP-LP transition, if recent coancestry, drift and/or ongoing gene flow between populations are masking the phenotypic signature of parallelism. We think multiple lines of evidence argue against this possibility. First, among the 12 populations with SNP data we found no correlation of pairwise genome wide F_{ST} values and phenotypic distance. Second, our use of mixed models to partition among-population variance suggest not only that neutral processes are insufficient to explain among-population differentiation, but also that adaptive divergence explains most variation (discussed further below). Third, and perhaps most importantly, when isolating the phenotypic change from HP to LP within rivers, the inferred directions of phenotypic evolution are not parallel among lineages. This analysis assumes that river can be used as a proxy for lineage (*sensu* de Lisle and Bolnick 2020), but that appears reasonable based on present and previous population genetic analyses (Willing *et al.* 2010; Blondel *et al.* 2020).

Thus, viewing male colour as a complex multivariate phenotype seen through the vision systems of biological agents of selection, we find no quantitative support for parallel evolution across the HP to LP regime transition. Rather, our results suggest that – in this phenotypic space – colour patterns evolve approximately independently in each river. However, the fact that genome wide molecular genetic structure does not predict phenotypic structuring argues against the idea that divergence of colour patterns could be primarily neutral. How can these results be reconciled with our existing understanding of colour evolution in guppies? In fact, we suggest the lack of parallelism, coupled to apparently greater variation among LP than among HP populations, is consistent with the widely-held view that reduced selection pressure from visual predators facilitates evolutionary divergence of male traits by female choice. In guppies, the evidence that females prefer more conspicuousness male patterns that also increase predation risk is abundant (reviewed in Houde 1997). However, this (univariate) conceptualisation of female choice masks the fact that, in multi-trait space, there may be many different directions that increase conspicuity to females.

621 The extent to which female choice drives Fisherian runaway evolution of traits that
622 are 'arbitrary' (not under viability selection) versus 'costly' has been extensively debated
623 (Kokko *et al.* 2002). However, even if females do prefer costly male phenotypes in all
624 populations, this need not translate into closely aligned vectors of sexual selection on
625 multivariate phenotype. Indeed, Endler and Houde (1995) demonstrated substantial
626 geographic variation in female preferences for colour patches, e.g. black, orange, and colour
627 contrast. Among-individual (female) differences in preference, a prerequisite for heritable
628 variation that would allow trait-preference coevolution, have also been demonstrated (Brooks
629 and Endler 2001; Brooks 2002). Lastly, we note that frequency dependent selection, with
630 females preferring novel male phenotypes is well documented in guppies (Hughes *et al.*
631 2013), and will generally impose vectors of directional selection that differ in space (i.e.
632 across populations) as well as time (e.g. as rare phenotypes become more common).
633 Our conclusion that predation regime has no consistent effect on the direction of
634 evolution in multivariate trait holds irrespective of the vision model used to define
635 phenotypes. However, the finding of population level correlations significantly less than +1
636 between homologous traits illustrates the wider potential for QPCA to offer new insights. The
637 same objective colour phenotype may be perceived differently by prospective mates and
638 potential predators. Here, guppy colour patterns appear generally more conspicuous in the
639 chromatic channel for conspecifics, whereas the pike cichlid is more sensitive to achromatic
640 (luminance) elements (Weadick *et al.* 2018). Such differences highlight the value of adopting
641 colour measures appropriate to the visual systems of hypothesised selective agents (Endler
642 1978; Endler *et al.* 2005; Endler and Mielke, 2005), and have implications for the way we the
643 evolution of colour signals with multiple receiving species. We also acknowledge however,
644 that that our study is naive to any abiotic factors (e.g., substrate, water colour, light
645 transmission, and canopy cover) that may affect *in situ* perception of phenotype by guppies
646 and/or their predators. Local abiotic conditions are an explicit part of the wider sensory drive
647 hypothesis (Endler 1980, 1992), and Kemp *et al.* (2018) found that canopy cover influenced
648 the relative abundance of iridescent versus melanic colour patches in guppies. While we

649 have no evidence to suggest this, it is at least possible that conditioning among-population
650 (or lineage) variance on abiotic covariates would reveal greater support for parallel evolution
651 in the colour phenotype as measured here.
652
653 **Insights from genome-scans and SNP associations**
654 Our pool-sequencing data provide several genetic insights that complement the phenotypic
655 analyses. First, based on detected associations with the phenotypic traits defined here, male
656 colour patterns are probably highly polygenic with genes distributed across the genome
657 rather than being restricted to the sex chromosomes or otherwise clustered. Associated
658 SNPs are found both outside and within genic regions, and involve cis-acting elements. For
659 instance, a SNP (LG:31463600) associated with differences in guppy-specific saturation was
660 found in an intergenic region near basonuclin 2 (*bnc2*), a gene implicated in the maintenance
661 of extracellular environments within which pigment cells driving patterning reside (Lang *et al.*
662 2009). Third, the minimal overlap between SNPs associated with homologous traits defined
663 under the two vision models is consistent with the population level phenotypic correlations
664 being less that one, suggesting that homolgous traits defined under different models are
665 genetically distinct. However, since colour genetics have often been studied using human
666 visual perception (Tripathi *et al.* 2009), it also highlights the possibility that ecologically-
667 important genes may have been previously overlooked. Conversely, we did not detect any
668 trait-SNP association consistency with colour genes previously identified in guppies, i.e.
669 *csf1ra* and *kita* (Kottler *et al.* 2013). This may again be explained by our choice of defined
670 phenotype; focusing here on measures of overall body patterns and/or conspicuity (as
671 perceived by selective agents), rather than features of individual pigmented patches (as
672 perceived by humans). Fourth, no SNPs significantly associated with tested covariables
673 were actually among the set identified as being significantly more differentiated than
674 expected under neutrality in the core BayPass model. Taken at face value, this could
675 indicate that greater (adaptive) genetic divergence among populations has occurred for
676 specific traits or aspects of phenotype (e.g. life history) that were not quantified in this study.

To our knowledge, this is the first study to investigate among-population natural variation in male guppy patterns at the genomic level. Consequently some brief, and necessarily tentative, comments on specific SNPs identified are perhaps warranted. Among those more differentiated than expected under neutrality, several SNPs were detected in the protein tyrosine phosphatase receptor of types *Fa* (*ptprfa*) and N2 (*ptprn2*). Basic functions of these genes include cell proliferation and epithelial cell-cell adhesion. They are considered to counteract tyrosinase kinase receptors (Xu and Fisher, 2012), which play known roles in melanocyte and melanophores development (*Kita* and *cKit*, respectively; Alexeev and Yoon 2006; Larsson and Parichy 2019). It is not known if tyrosine phosphatase receptors carry a direct pigmentation function, although this is plausible given their documented involvement in cell differentiation, oncogenic- events, and sensory guidance to the skin (Wang *et al.*2012). Several SNPs deviating from neutral expectaions were also identified in less well-known genes including *polg* and *trio,* which are part of regulatory networks influencing melanocyte differentiation (Seberg *et al.* 2017; Park *et al.* 2018). Among SNPs associated with tested covariates (trait means and predation regime), we also find several in (or near) genes with known roles in fish colour. For instance, one SNP association with guppy vision $sat_{\Delta S}$ was near *ablim3*, a gene thought to be involved in pigment cell movement in fishes (Ahi *et al.* 2020). Another was found within *cx30.3*, part of a family of genes implicated in zebrafish skin development and pattern formation (Tao *et al.* 2010; Irion *et al.* 2014).

Conclusion

Trinidadian guppies ostensibly represent a classic example of parallel (or convergent) evolution, with repeated divergence in male colour patterns between upstream and downstream populations due partly to predation conditions. We find that the well-described tendency for greater conspicuousness under low predation holds qualitatively true when we analyse single traits defined under guppy and predator vision models. However, statistical support for this is weak, and repeated colonisation of low predation habitats has

not lead to the parallel evolution of conspicuous phenotypes when these are characterised in quantitative, multivariate, phenotypic space. Instead, we suggest that colonisation of LP habitat may reduce selective constraints on phenotypic space imposed by predation, facilitating population-specific divergence under sexual selection. Together, our results are nonetheless consistent with the standard view that reduced selection by predators allows male colour traits to evolve under sexual selection imposed by female choice. However, the common assertion that female choice in guppies selects for 'brighter' or more 'conspicuous' males, masks the fact that – in multivariate trait space - colour is evolving in rather different directions across populations and lineages.

ACKNOWLEDGEMENTS

This work was supported by a BBSRC grant to AJW (BB/L022656/1), a Genetics Society (UK) Grant to LY and a European Research Council Advanced Grant 695225 (GUPPYSEX) awarded to D. Charlesworth (with AJW and DC as co-investigators). We thank D. Charlesworth for comments on an earlier version of this MS. We also thank R. Mahabir, R. Heathcote for assistance with the field collection and Trinidad-UK shipment of guppies. Guppy collection was approved by Trinidad's Ministry of Agriculture, Land and Fisheries and import to the UK was approved by CEFAS (EW087-O-816A).

REFERENCES

Ahi, E. P., Lecaudey, L. A., Ziegelbecker, A., Steiner, O., Glabonjat, R., Goessler, W., … Sefc, K. M. (2020). Comparative transcriptomics reveals candidate carotenoid color genes in an East African cichlid fish. *BMC Genomics*, *21*. doi: 10.1186/s12864-020-6473-8

Alexeev, V., & Yoon, K. (2006). Distinctive role of the cKit receptor tyrosine kinase signaling in mammalian melanocytes. *The Journal of Investigative Dermatology*, *126*(5), 1102–1110. doi: 10.1038/sj.jid.5700125

Allender, C. J., Seehausen, O., Knight, M. E., Turner, G. F., & Maclean, N. (2003). Divergent selection during speciation of Lake Malawi cichlid fishes inferred from parallel radiations in nuptial coloration. *Proceedings of the National Academy of Sciences*, *100*(24), 14074–14079. doi: 10.1073/pnas.2332665100

Ashburner, M., Ball, C. A., Blake, J. A., Botstein, D., Butler, H., Cherry, J. M., … Sherlock, G. (2000). Gene ontology: tool for the unification of biology. The Gene Ontology Consortium. *Nature Genetics*, *25*(1), 25–29. doi: 10.1038/75556

739 Astles, P. A., Moore A. J., & Preziosi R. F. (2006). A comparison of methods to estimate
740 cross-environment genetic correlations. *Journal of Evolutionary Biology* 19(1): 114-
741 122. doi: 10.1111/j.1420-9101.2005.00997.x.
742 Belleghem, S. M. V., Papa, R., Ortiz-Zuazaga, H., Hendrickx, F., Jiggins, C. D., McMillan, W.
743 O., & Counterman, B. A. (2018). patternize: An R package for quantifying colour
744 pattern variation. *Methods in Ecology and Evolution*, *9*(2), 390–398. doi:
745 10.1111/2041-210X.12853
746 Blondel, L., Baillie, L., Quinton, J., Alemu, J. B., Paterson, I., Hendry, A. P., & Bentzen, P.
747 (2019). Evidence for contemporary and historical gene flow between guppy
748 populations in different watersheds, with a test for associations with adaptive traits.
749 *Ecology and Evolution*, *9*(8), 4504–4517. doi: 10.1002/ece3.5033
750 Bolnick, D. I., Barrett, R. D. H., Oke, K. B., Rennison, D. J., & Stuart, Y. E. (2018).
751 (Non)Parallel Evolution. *Annual Review of Ecology, Evolution, and Systematics*,
752 *49*(1), 303–330. doi: 10.1146/annurev-ecolsys-110617-062240
753 Brooks, R., & Endler, J. A. (2001). Female guppies agree to differ: phenotypic and genetic
754 variation in mate-choice behavior and the consequences for sexual selection.
755 *Evolution* 55(8), 1644–1655. doi: 10.1111/j.0014-3820.2001.tb00684.x
756 Brooks, Robert. (2002). Variation in female mate choice within guppy populations: population
757 divergence, multiple ornaments and the maintenance of polymorphism. *Genetica*,
758 *116*(2–3), 343–358.
759 Butler, D., Cullis, B., Gilmour, A., Gogel, B., & Thompson, R. (2017). *ASReml-R Reference*
760 *Manual Version 4*. Hemel Hempstead, HP1 1ES, UK: VSN International Ltd.
761 Butlin, R. K., Saura, M., Charrier, G., Jackson, B., André, C., Caballero, A., … Rolán-
762 Alvarez, E. (2014). Parallel evolution of local adaptation and reproductive isolation in
763 the face of gene flow. *Evolution; International Journal of Organic Evolution*, *68*(4),
764 935–949. doi: 10.1111/evo.12329
765 Caves, E. M., Sutton, T. T., & Johnsen, S. (2017). Visual acuity in ray-finned fishes
766 correlates with eye size and habitat. *The Journal of Experimental Biology*, *220*(Pt 9),
767 1586–1596. doi: 10.1242/jeb.151183
768 Cole, G. L., & Endler, J. A. (2015). Variable environmental effects on a multicomponent
769 sexually selected trait. *The American Naturalist*, *185*(4), 452–468. doi:
770 10.1086/680022
771 Cuthill, I. C., Allen, W. L., Arbuckle, K., Caspers, B., Chaplin, G., Hauber, M. E., … Caro, T.
772 (2017). The biology of color. *Science*, *357*(6350). doi: 10.1126/science.aan0221
773 De Lisle, S. P. D., & Bolnick, D. I. (2020). A multivariate view of parallel evolution. *Evolution*,
774 *74*(7), 1466–1481. doi: 10.1111/evo.14035
775 Dick, C., Hinh, J., Hayashi, C. Y., & Reznick, D. N. (2018). Convergent evolution of
776 coloration in experimental introductions of the guppy (Poecilia reticulata). *Ecology*
777 *and Evolution*, *8*(17), 8999–9006. doi: 10.1002/ece3.4418
778 Dyer, A. G., Boyd-Gerny, S., McLoughlin, S., Rosa, M. G. P., Simonov, V., & Wong, B. B. M.
779 (2012). Parallel evolution of angiosperm colour signals: common evolutionary
780 pressures linked to hymenopteran vision. *Proceedings. Biological Sciences*,
781 *279*(1742), 3606–3615. doi: 10.1098/rspb.2012.0827
782 Elmer, K. R., & Meyer, A. (2011). Adaptation in the age of ecological genomics: insights from
783 parallelism and convergence. *Trends in Ecology & Evolution*, *26*(6), 298–306. doi:
784 10.1016/j.tree.2011.02.008
785 Endler, J. A. (1978). A Predator's View of Animal Color Patterns. *Evolutionary Biology*, 319–
786 364. doi: 10.1007/978-1-4615-6956-5_5
787 Endler, J. A. (1980). Natural Selection on Color Patterns in Poecilia reticulata. *Evolution*,
788 *34*(1), 76–91. JSTOR. doi: 10.2307/2408316
789 Endler, J. A. (1983). Natural and secual selection on color patterns in poeciliids fishers.
790 *Environment Biology of Fishes* 9(2), 173-190.
791 Endler, J. A. (1991). Variation in the appearance of guppy color patterns to guppies and their
792 predators under different visual conditions. *Vision Research*, *31*(3), 587–608. doi:
793 10.1016/0042-6989(91)90109-i

Endler, J. A. (1992). Signals, Signal Conditions, and the Direction of Evolution. *The American Naturalist*, *139*, S125–S153. doi: 10.1086/285308

Endler, J. A. (1995). Multiple-trait coevolution and environmental gradients in guppies. *Trends in Ecology & Evolution*, *10*(1), 22–29. doi: 10.1016/s0169-5347(00)88956-9

Endler, J. A. (2012). A framework for analysing colour pattern geometry: adjacent colours. *Biological Journal of the Linnean Society*, *107*(2), 233–253. doi: 10.1111/j.1095-8312.2012.01937.x

Endler, J. A. (2015). Signals, Signal Conditions, and the Direction of Evolution. *The American Naturalist*. (world). doi: 10.1086/285308

Endler, J. A., Cole, G. L., & Kranz, A. M. (2018). Boundary strength analysis: Combining colour pattern geometry and coloured patch visual properties for use in predicting behaviour and fitness. *Methods in Ecology and Evolution*, *9*(12), 2334–2348. doi: 10.1111/2041-210X.13073

Endler, J. A., & Houde, A. E. (1995). Geographic variation in female preferences for male traits in poecilia reticulata. *Evolution*, *49*(3), 456–468. doi: 10.1111/j.1558-5646.1995.tb02278.x

Endler, J. A., & Mappes, J. (2017). The current and future state of animal coloration research. *Philosophical Transactions of the Royal Society of London. Series B, Biological Sciences*, *372*(1724). doi: 10.1098/rstb.2016.0352

Endler, J. A., & Mielke, P. W. (2005). Comparing entire colour patterns as birds see them. *Biological Journal of the Linnean Society*, *86*(4), 405–431. doi: 10.1111/j.1095-8312.2005.00540.x

Fraser, B. A., Künstner, A., Reznick, D. N., Dreyer, C., & Weigel, D. (2015). Population genomics of natural and experimental populations of guppies (Poecilia reticulata). *Molecular Ecology*, *24*(2), 389–408. doi: 10.1111/mec.13022

Funk, D. J., Egan, S. P., & Nosil, P. (2011). Isolation by adaptation in Neochlamisus leaf beetles: host-related selection promotes neutral genomic divergence. *Molecular Ecology*, *20*(22), 4671–4682. doi: 10.1111/j.1365-294X.2011.05311.x

Gautier, M. (2015). Genome-Wide Scan for Adaptive Divergence and Association with Population-Specific Covariates. *Genetics*, *201*(4), 1555–1579. doi: 10.1534/genetics.115.181453

Gautier, M., Foucaud, J., Gharbi, K., Cézard, T., Galan, M., Loiseau, A., … Estoup, A. (2013). Estimation of population allele frequencies from next-generation sequencing data: pool-versus individual-based genotyping. *Molecular Ecology*, *22*(14), 3766–3779. doi: 10.1111/mec.12360

Gautier, M., Yamaguchi, J., Foucaud, J., Loiseau, A., Ausset, A., Facon, B., … Prud'homme, B. (2018). The Genomic Basis of Color Pattern Polymorphism in the Harlequin Ladybird. *Current Biology: CB*, *28*(20), 3296-3302.e7. doi: 10.1016/j.cub.2018.08.023

Gotanda, K. M., Pack, A., LeBlond, C., & Hendry, A. P. (2019). Do replicates of independent guppy lineages evolve similarly in a predator-free laboratory environment? *Ecology and Evolution*, *9*(1), 36–51. doi: 10.1002/ece3.4585

Günther, T., & Coop, G. (2013). Robust identification of local adaptation from allele frequencies. *Genetics*, *195*(1), 205–220. doi: 10.1534/genetics.113.152462

Hartl, D. L., & Clark, A. G. (1997). *Principles of population genetics*. Sinauer Associates.

Haskins, C. P., Haskins, E. F., McLaughlin, J. J., & Hewitt, R. E. (1961). Polymorphism and population structure in Lebistes reticulatus, an ecological study. In *Vertebrate Speciation* (W. F. Blair, pp. 320–395). Austin: University of Texas Press.

Houde, A. (1997). *Sex, Color, and Mate Choice in Guppies* (Vol. 71). Princeton University Press. JSTOR. doi: 10.2307/j.ctvs32rtk

Howe, K., Clark, M. D., Torroja, C. F., Torrance, J., Berthelot, C., Muffato, M., … Stemple, D. L. (2013). The zebrafish reference genome sequence and its relationship to the human genome. *Nature*, *496*(7446), 498–503. doi: 10.1038/nature12111

Hughes, K. A., Houde, A. E., Price, A. C., & Rodd, F. H. (2013). Mating advantage for rare males in wild guppy populations. *Nature*, *503*(7474), 108–110. doi: 10.1038/nature12717

Irion, U., Frohnhöfer, H. G., Krauss, J., Champollion, T. Ç., Maischein, H.-M., Geiger-Rudolph, S., … Nüsslein-Volhard, C. (2014, December 23). Gap junctions composed of connexins 41.8 and 39.4 are essential for colour pattern formation in zebrafish. doi: 10.7554/eLife.05125

Karim, N., Gordon, S. P., Schwartz, A. K., & Hendry, A. P. (2007). This is not déjà vu all over again: male guppy colour in a new experimental introduction. *Journal of Evolutionary Biology*, *20*(4), 1339–1350. doi: 10.1111/j.1420-9101.2007.01350.x

Kawamura, S., Kasagi, S., Kasai, D., Tezuka, A., Shoji, A., Takahashi, A., … Kawata, M. (2016). Spectral sensitivity of guppy visual pigments reconstituted in vitro to resolve association of opsins with cone cell types. *Vision Research*, *127*, 67–73. doi: 10.1016/j.visres.2016.06.013

Kemp, D. J., Batistic, F.-K., & Reznick, D. N. (2018). Predictable adaptive trajectories of sexual coloration in the wild: Evidence from replicate experimental guppy populations*. *Evolution*, *72*(11), 2462–2477. doi: 10.1111/evo.13564

Kemp, D. J., Reznick, D. N., Grether, G. F., & Endler, J. A. (2009). Predicting the direction of ornament evolution in Trinidadian guppies (Poecilia reticulata). *Proceedings of the Royal Society B: Biological Sciences*. (world). doi: 10.1098/rspb.2009.1226

Kofler, R., Pandey, R. V., & Schlötterer, C. (2011). PoPoolation2: identifying differentiation between populations using sequencing of pooled DNA samples (Pool-Seq). *Bioinformatics*, *27*(24), 3435–3436. doi: 10.1093/bioinformatics/btr589

Kokko, H., Brooks, R., McNamara, J. M., & Houston, A. I. (2002). The sexual selection continuum. *Proceedings of the Royal Society of London. Series B: Biological Sciences*. (world). doi: 10.1098/rspb.2002.2020

Kottler, V. A., Fadeev, A., Weigel, D., & Dreyer, C. (2013). Pigment pattern formation in the guppy, Poecilia reticulata, involves the Kita and Csf1ra receptor tyrosine kinases. *Genetics*, *194*(3), 631–646. doi: 10.1534/genetics.113.151738

Kranz, A. M., Cole, G. L., Singh, P., & Endler, J. A. (2018). Colour pattern component phenotypic divergence can be predicted by the light environment. *Journal of Evolutionary Biology*, *31*(10), 1459–1476. doi: 10.1111/jeb.13342

Kranz, A. M., Forgan, L. G., Cole, G. L., & Endler, J. A. (2018). Light environment change induces differential expression of guppy opsins in a multi-generational evolution experiment. *Evolution* 72(8), 1656-1676. doi: 10.1111/evo.13519

Kratochwil, C. F., Liang, Y., Gerwin, J., Woltering, J. M., Urban, S., Henning, F., … Meyer, A. (2018). Agouti-related peptide 2 facilitates convergent evolution of stripe patterns across cichlid fish radiations. *Science (New York, N.Y.)*, *362*(6413), 457–460. doi: 10.1126/science.aao6809

Künstner, A., Hoffmann, M., Fraser, B. A., Kottler, V. A., Sharma, E., Weigel, D., & Dreyer, C. (2016). The Genome of the Trinidadian Guppy, Poecilia reticulata, and Variation in the Guanapo Population. *PloS One*, *11*(12), e0169087. doi: 10.1371/journal.pone.0169087

Lang, M. R., Patterson, L. B., Gordon, T. N., Johnson, S. L., & Parichy, D. M. (2009). Basonuclin-2 Requirements for Zebrafish Adult Pigment Pattern Development and Female Fertility. *PLOS Genetics*, *5*(11), e1000744. doi: 10.1371/journal.pgen.1000744

Laver, C. R. J., & Taylor, J. S. (2011). RT-qPCR reveals opsin gene upregulation associated with age and sex in guppies (Poecilia reticulata) - a species with color-based sexual selection and 11 visual-opsin genes. *BMC Evolutionary Biology*, *11*, 81. doi: 10.1186/1471-2148-11-81

Leinonen, T., McCairns, R. J. S., O'Hara, R. B., & Merilä, J. (2013). Q ST – F ST comparisons: evolutionary and ecological insights from genomic heterogeneity. *Nature Reviews Genetics*, *14*(3), 179–190. doi: 10.1038/nrg3395

Li, H., & Durbin, R. (2010). Fast and accurate long-read alignment with Burrows-Wheeler transform. *Bioinformatics (Oxford, England)*, *26*(5), 589–595. doi: 10.1093/bioinformatics/btp698

Li, H., Handsaker, B., Wysoker, A., Fennell, T., Ruan, J., Homer, N., … 1000 Genome Project Data Processing Subgroup. (2009). The Sequence Alignment/Map format and SAMtools. *Bioinformatics (Oxford, England)*, *25*(16), 2078–2079. doi: 10.1093/bioinformatics/btp352

Lindholm A, Breden F. (2002). Sex chromosomes and sexual selection in Poeciliid Fishes. *American Naturalist* 160, S214-224.

Long, K. D. (n.d.). *Variation in mating behavior of the guppy, Poecilia reticulata, as a function of environmental, irradiance, visual acuity, and perception of male color patern (Doctoral dissertation).* Berkeley CA: University of California.

Magurran, A. E. (n.d.). *Evolutionary Ecology: The Trinidadian Guppy*. Oxford University Press.

Martin, R. A., Riesch, R., Heinen-Kay, J. L., & Langerhans, R. B. (2014). Evolution of male coloration during a post-Pleistocene radiation of Bahamas mosquitofish (*Gambusia hubbsi)*. *Evolution*, *68*(2), 397–411. doi: 10.1111/evo.12277

McKinnon, J. S., Mori, S., Blackman, B. K., David, L., Kingsley, D. M., Jamieson, L., … Schluter, D. (2004). Evidence for ecology's role in speciation. *Nature*, *429*(6989), 294–298. doi: 10.1038/nature02556

Millar, N. P., Reznick, D. N., Kinnison, M. T., & Hendry, A. P. (2006). Disentangling the selective factors that act on male colour in wild guppies. *Oikos*, *113*(1), 1–12. doi: 10.1111/j.0030-1299.2006.14038.x

Montenegro, J., Mochida, K., Matsui, K., Mokodongan, D. F., Sumarto, B. K. A., Lawelle, S. A., … Yamahira, K. (2019). Convergent evolution of body color between sympatric freshwater fishes via different visual sensory evolution. *Ecology and Evolution*, *9*(11), 6389–6398. doi: 10.1002/ece3.5211

Nosil, P., Egan, S. P., & Funk, D. J. (2008). Heterogeneous genomic differentiation between walking-stick ecotypes: "isolation by adaptation" and multiple roles for divergent selection. *Evolution; International Journal of Organic Evolution*, *62*(2), 316–336. doi: 10.1111/j.1558-5646.2007.00299.x

Nosil, P., Funk, D. J., & Ortiz-Barrientos, D. (2009). Divergent selection and heterogeneous genomic divergence. *Molecular Ecology*, *18*(3), 375–402. doi: 10.1111/j.1365-294X.2008.03946.x

Olendorf, R., Rodd, F. H., Punzalan, D., Houde, A. E., Hurt, C., Reznick, D. N., & Hughes, K. A. (2006). Frequency-dependent survival in natural guppy populations. *Nature*, *441*(7093), 633–636. doi: 10.1038/nature04646

Park, J. J., Diefenbach, R. J., Joshua, A. M., Kefford, R. F., Carlino, M. S., & Rizos, H. (2018). Oncogenic signaling in uveal melanoma. *Pigment Cell & Melanoma Research*, *31*(6), 661–672. doi: 10.1111/pcmr.12708

Pascoal, S., Mendrok, M., Mitchell, C., Wilson, A. J., Hunt, J., & Bailey, N. W. (2016). Sexual selection and population divergence I: The influence of socially flexible cuticular hydrocarbon expression in male field crickets (Teleogryllus oceanicus). *Evolution*, *70*(1), 82–97. doi: 10.1111/evo.12839

Pascoal, S., Mendrok, M., Wilson, A. J., Hunt, J., & Bailey, N. W. (2017). Sexual selection and population divergence II. Divergence in different sexual traits and signal modalities in field crickets (Teleogryllus oceanicus). *Evolution*, *71*(6), 1614–1626. doi: 10.1111/evo.13239

Patterson, L. B., & Parichy, D. M. (2019). Zebrafish Pigment Pattern Formation: Insights into the Development and Evolution of Adult Form. *Annual Review of Genetics*, *53*, 505–530. doi: 10.1146/annurev-genet-112618-043741

Pujol, B., Wilson, A. J., Ross, R. I. C., & Pannell, J. R. (2008). Are QST–FST comparisons for natural populations meaningful? *Molecular Ecology*, *17*(22), 4782–4785. doi: 10.1111/j.1365-294X.2008.03958.x

R Core Team. (2019). R: A language and environment for statistical computing. Retrieved June 10, 2020, from R Foundation for Statistical Computing, Vienna, Austria website: https://www.r-project.org/

Räsänen, K., & Hendry, A. P. (2008). Disentangling interactions between adaptive divergence and gene flow when ecology drives diversification. *Ecology Letters*, *11*(6), 624–636. doi: 10.1111/j.1461-0248.2008.01176.x

Rasband, W. S. (1997). *ImageJ*. Bethesda, Maryland, USA: U. S. National Institutes of Health. Retrieved from https://imagej.nih.gov/ij/

Reznick, D. N. (1997). Life history evolution in guppies (Poecilia reticulata): guppies as a model for studying the evolutionary biology of aging. *Experimental Gerontology*, *32*(3), 245–258. doi: 10.1016/s0531-5565(96)00129-5

Reznick, David N., Butler, M. J., Rodd, F. H., & Ross, P. (1996). Life-history evolution in guppies (*Poecilia reticulata*) 6. Differential mortality as a mechanism for natural selection. *Evolution*, *50*(4), 1651–1660. doi: 10.1111/j.1558-5646.1996.tb03937.x

Schlötterer, C., Tobler, R., Kofler, R., & Nolte, V. (2014a). Sequencing pools of individuals - mining genome-wide polymorphism data without big funding. *Nature Reviews. Genetics*, *15*(11), 749–763. doi: 10.1038/nrg3803

Schluter, D., Clifford, E. A., Nemethy, M., & McKinnon, J. S. (2004). Parallel evolution and inheritance of quantitative traits. *The American Naturalist*, *163*(6), 809–822. doi: 10.1086/383621

Seberg, H. E., Van Otterloo, E., Loftus, S. K., Liu, H., Bonde, G., Sompallae, R., … Cornell, R. A. (2017). TFAP2 paralogs regulate melanocyte differentiation in parallel with MITF. *PLoS Genetics*, *13*(3). doi: 10.1371/journal.pgen.1006636

Seehausen, O., Terai, Y., Magalhaes, I. S., Carleton, K. L., Mrosso, H. D. J., Miyagi, R., … Okada, N. (2008). Speciation through sensory drive in cichlid fish. *Nature*, *455*(7213), 620–626. doi: 10.1038/nature07285

Sibeaux, A., Cole, G. L., & Endler, J. A. (2019). Success of the receptor noise model in predicting colour discrimination in guppies depends upon the colours tested. *Vision Research*, *159*, 86–95. doi: 10.1016/j.visres.2019.04.002

Steiner, C. C., Römpler, H., Boettger, L. M., Schöneberg, T., & Hoekstra, H. E. (2009). The Genetic Basis of Phenotypic Convergence in Beach Mice: Similar Pigment Patterns but Different Genes. *Molecular Biology and Evolution*, *26*(1), 35–45. doi: 10.1093/molbev/msn218

Stevens, M., Párraga, C. A., Cuthill, I. C., Partridge, J. C., & Troscianko, T. S. (2007). Using digital photography to study animal coloration. *Biological Journal of the Linnean Society*, *90*(2), 211–237. doi: 10.1111/j.1095-8312.2007.00725.x

Stram, Daniel O., & Lee, J. W. (1994). Variance Components Testing in the Longitudinal Mixed Effects Model. *Biometrics*, *50*(4), 1171–1177. JSTOR. doi: 10.2307/2533455

Stuart, Y. E., Veen, T., Weber, J. N., Hanson, D., Ravinet, M., Lohman, B. K., … Bolnick, D. I. (2017). Contrasting effects of environment and genetics generate a continuum of parallel evolution. *Nature Ecology & Evolution*, *1*(6), 158. doi: 10.1038/s41559-017-0158

Suk, H. Y., & Neff, B. D. (2009). Microsatellite genetic differentiation among populations of the Trinidadian guppy. *Heredity*, *102*(5), 425–434. doi: 10.1038/hdy.2009.7

Tao, L., DeRosa, A. M., White, T. W., & Valdimarsson, G. (2010). Zebrafish cx30.3: Identification and Characterization of a Gap Junction Gene Highly Expressed in the Skin. *Developmental Dynamics : An Official Publication of the American Association of Anatomists*, *239*(10), 2627–2636. doi: 10.1002/dvdy.22399

The Gene Ontology Consortium. (2019). The Gene Ontology Resource: 20 years and still GOing strong. *Nucleic Acids Research*, *47*(D1), D330–D338. doi: 10.1093/nar/gky1055

Tripathi, N., Hoffmann, M., Willing, E.-M., Lanz, C., Weigel, D., & Dreyer, C. (2009). Genetic linkage map of the guppy, Poecilia reticulata, and quantitative trait loci analysis of male size and colour variation. *Proceedings. Biological Sciences*, *276*(1665), 2195–2208. doi: 10.1098/rspb.2008.1930

Troscianko, J., & Stevens, M. (2015). Image calibration and analysis toolbox – a free software suite for objectively measuring reflectance, colour and pattern. *Methods in Ecology and Evolution*, *6*(11), 1320–1331. doi: 10.1111/2041-210X.12439

van den Berg, C. P., Troscianko, J., Endler, J. A., Marshall, N. J., & Cheney, K. L. (2020). Quantitative Colour Pattern Analysis (QCPA): A comprehensive framework for the analysis of colour patterns in nature. *Methods in Ecology and Evolution*, *11*(2), 316–332. doi: 10.1111/2041-210X.13328

Vorobyev, M., & Osorio, D. (1998). Receptor noise as a determinant of colour thresholds. *Proceedings. Biological Sciences*, *265*(1394), 351–358. doi: 10.1098/rspb.1998.0302

Wang, F., Wolfson, S. N., Gharib, A., & Sagasti, A. (2012). LAR receptor tyrosine phosphatases and HSPGs guide peripheral sensory axons to the skin. *Current Biology: CB*, *22*(5), 373–382. doi: 10.1016/j.cub.2012.01.040

Weadick, C. J., Loew, E. R., Rodd, F. H., & Chang, B. S. W. (2012). Visual pigment molecular evolution in the Trinidadian pike cichlid (Crenicichla frenata): a less colorful world for neotropical cichlids? *Molecular Biology and Evolution*, *29*(10), 3045–3060. doi: 10.1093/molbev/mss115

Whitlock, M. C., & Guillaume, F. (2009). Testing for Spatially Divergent Selection: Comparing QST to FST. *Genetics*, *183*(3), 1055–1063. doi: 10.1534/genetics.108.099812

Willing, E.-M., Bentzen, P., van Oosterhout, C., Hoffmann, M., Cable, J., Breden, F., … Dreyer, C. (2010). Genome-wide single nucleotide polymorphisms reveal population history and adaptive divergence in wild guppies. *Molecular Ecology*, *19*(5), 968–984. doi: 10.1111/j.1365-294X.2010.04528.x

Xu, Y., & Fisher, G. J. (2012). Receptor type protein tyrosine phosphatases (RPTPs) – roles in signal transduction and human disease. *Journal of Cell Communication and Signaling*, *6*(3), 125–138. doi: 10.1007/s12079-012-0171-5

Young, M. J., Simmons, L. W., & Evans, J. P. (2011). Predation is associated with variation in colour pattern, but not body shape or colour reflectance, in a rainbowfish (Melanotaenia australis). *The Journal of Animal Ecology*, *80*(1), 183–191. doi: 10.1111/j.1365-2656.2010.01759.x

DATA ACCESSIBILITY

Raw phenotypic and genomic data as well as R and Java scripts will be available publicly upon the acceptance of the manuscript in Dryad, GeneBank, and appropriate data repositories.

AUTHOR CONTRIBUTIONS

LY and AW designed the study with input from DPC and JT. LY, DPC and AW performed the research. JT and IR contributed analytical tools. LY and AW analysed the data. LY and AW wrote the paper with input from DCP, IR, and JT.

TABLES AND FIGURES

Table 1. Description of collection site (drainage, river, and regime type) and their GPS coordinates. Sample size denotes fish that were photographed.

Drainage	River	Regime	Site code	Lat (N)	Long (W)	n_{males}
Caroni	Aripo	high	AH	10° 39' 02"	61° 13' 26"	26
Caroni	Aripo	low	AL	10° 41' 08"	61° 13' 56"	29
Caroni	Aripo	low	AL2	10° 41' 10"	61° 13’ 30"	23
Caroni	Guanapo	high	GH	10° 39' 28"	61° 15' 13"	26
Caroni	Guanapo	low	GL	10° 42' 42"	61° 16' 01"	5
Caroni	Guanapo	low	GL2	10° 42' 20"	61° 15' 48"	26
Northern	Marianne	high	MH	10° 45' 54"	61° 18' 15"	25
Northern	Marianne	low	ML	10° 44’ 58"	61° 17' 13"	23
Northern	Marianne	low	PML	10° 46’ 40"	61° 18' 04"	28
Northern	Paria	low	PL	10° 44’ 57"	61° 15' 54"	24
Northern	Yarra	high	YH	10° 47' 23"	61° 21’ 12"	24
Northern	Yarra	low	YL	10° 44' 25"	61° 19’ 17"	26
Oropouche	Quare	high	QH	10° 39' 53"	61° 11' 35"	27
Oropouche	Quare	low	QL	10° 40’ 33"	61° 11’ 49"	26
Oropouche	Turure	high	TH	10° 40' 32"	61° 09' 54"	26
Oropouche	Turure	low	TL	10° 41' 31"	61° 10' 18"	24

Table 2. Estimated regime (fixed) and population (random) effects from univariate mixed models of each trait. Regime effects denote the consequence of low relative to high predation regime with inference by F-tests. Among-population variance (V_{Pop}) is conditional on fixed effects and was tested by likelihood ratio test. Also shown is the population level repeatability (R_{Pop}).

Vision model	Trait	Fixed effects				Random effects			
		Regime (SE)	F	DF	P	V_{Pop} (SE)	R_{Pop} (SE)	$X^2_{0,1}$	P
Guppy	sat_{DS}	0.148 (0.353)	0.177	1,13.9	0.681	0.439 (0.177)	0.418 (0.1)	150	<0.001
	lum_{DS}	0.833 (0.366)	5.171	1,13.7	0.04	0.484 (0.192)	0.539 (0.1)	204	<0.001
	$chrom_{DS}$	0.271 (0.434)	0.39	1,14	0.543	0.689 (0.267)	0.638 (0.091)	307	<0.001
	CoV_{DS}	0.230 (0.302)	0.58	1,13.8	0.459	0.307 (0.130)	0.301 (0.091)	80.5	<0.001
Cichlid	sat_{DS}	0.270 (0.449)	0.361	1,14	0.557	0.744 (0.286)	0.713 (0.08)	403	<0.001
	lum_{DS}	0.054 (0.401)	0.018	1,13.7	0.896	0.578 (0.230)	0.514 (0.101)	186	<0.001
	$chrom_{DS}$	0.570 (0.433)	1.728	1,14	0.21	0.690 (0.266)	0.682 (0.085)	357	<0.001
	CoV_{DS}	0.245 (0.400)	0.375	1,13.2	0.551	0.556 (0.231)	0.512 (0.106)	136	<0.001

Table 3. Estimates of among-population repeatabilities (R_{Pop}) derived from univariate mixed models that partition total population effects into components attributable to putative neutral ($R_{Pop.N}$) versus selective ($R_{Pop.S}$) processes. Also shown are LRT comparisons to a reduced model in which all among-population variance is assumed to have a neutral basis. Note where a variance component, and so the corresponding repeatability, was bound to zero to keep it in allowable parameter space no estimate of the SE is possible.

Vision model	Trait	R_{Pop} (SE)	$R_{Pop.N}$ (SE)	$R_{Pop.S}$ (SE)	$X^2_{0,1}$	P
Guppy	sat_{DS}	0.385 (0.109)	0.000 (-)	0.385 (0.109)	3.787	0.026
	lum_{DS}	0.414 (0.144)	0.073 (0.083)	0.342 (0.196)	4.537	0.017
	$chrom_{DS}$	0.654 (0.136)	0.031 (0.092)	0.623 (0.208)	4.95	0.013
	cov_{DS}	0.240 (0.089)	0.000 (-)	0.240 (0.089)	9.651	0.001
Cichlid	sat_{DS}	0.418 (0.109)	0.418 (0.109)	0.000 (-)	0	0.5
	lum_{DS}	0.364 (0.108)	0.000 (-)	0.364 (0.108)	5.286	0.011
	$chrom_{DS}$	0.400 (0.108)	0.400 (0.108)	0.000 (-)	0	0.5
	cov_{DS}	0.495 (0.114)	0.000 (-)	0.495 (0.114)	8.581	0.002

Table 4. Spectral decomposition for among independent lineages for phenotypic parallelism. Note: Highlighted cells indicates that that dimension is significantly above 95% threshold.

(a) guppy-vision colour

		Eigenvectors								
		q1	***q2***	***q3***	***q4***	***q5***	***q6***	***q7***	***q8***	***q9***
	eigenvalues (upper 95%)	5.06	3.25	2.13	1.26	0.00	0.00	0.00	0.00	0.00
	eigenvalues (obs)	4.97	3.38	0.40	0.26	0.00	0.00	0.00	0.00	0.00
	% Variance explained	0.55	0.38	0.04	0.03	0.00	0.00	0.00	0.00	0.00
lineage	aripo	-0.43	0.08	-0.13	0.50	0.72	0.00	0.00	0.00	0.17
	aripo1	-0.41	0.17	0.29	-0.30	0.05	-0.01	0.71	-0.23	-0.25
	guanapo	0.35	0.29	-0.46	-0.18	0.21	-0.56	0.32	0.28	0.04
	guanapo1	0.18	-0.48	-0.20	0.45	-0.07	0.18	0.40	0.24	-0.50
	marianne	-0.07	0.52	-0.32	-0.16	0.08	0.44	-0.26	0.10	-0.56
	marianne1	0.01	0.50	0.47	0.51	-0.29	-0.26	-0.02	0.32	-0.12
	quare	-0.42	-0.16	0.01	-0.28	-0.08	0.13	0.01	0.80	0.21
	turure	-0.38	-0.28	-0.04	-0.10	-0.02	-0.61	-0.38	-0.07	-0.49
	yarra	-0.40	0.14	-0.56	0.24	-0.58	-0.03	0.12	-0.21	0.23

(b) cichlid-vision colour

		Eigenvectors								
		q1	***q2***	***q3***	***q4***	***q5***	***q6***	***q7***	***q8***	***q9***
	eigenvalues (upper 95%)	5.06	3.19	2.12	1.26	0.00	0.00	0.00	0.00	0.00
	eigenvalues	4.59	2.42	1.85	0.14	0.00	0.00	0.00	0.00	0.00
	% Variance explained	0.51	0.27	0.21	0.02	0.00	0.00	0.00	0.00	0.00
lineage	aripo	-0.16	0.56	-0.25	0.19	0.57	0.00	0.00	0.00	0.48
	aripo1	-0.43	0.20	0.10	-0.42	0.32	-0.37	0.21	-0.12	-0.54
	guanapo	-0.38	-0.34	-0.17	-0.32	-0.03	-0.29	-0.17	0.61	0.35
	guanapo1	0.09	-0.50	-0.44	0.03	0.22	-0.37	-0.08	-0.59	0.12
	marianne	-0.28	0.02	-0.59	-0.15	-0.29	0.43	0.53	-0.06	-0.01
	marianne1	-0.41	0.26	-0.18	0.02	-0.36	0.09	-0.72	-0.26	-0.11

	quare	0.44	0.08	-0.10	-0.76	0.20	0.32	-0.26	-0.05	0.06
	turure	0.33	0.44	-0.14	-0.16	-0.50	-0.59	0.16	-0.03	0.17
	yarra	-0.31	-0.06	0.54	-0.25	-0.16	0.09	0.18	-0.44	0.54

(c) Combined

		Eigenvectors								
		q1	***q2***	***q3***	***q4***	***q5***	***q6***	***q7***	***q8***	***q9***
	eigenvalues (upper 95%)	3.66	2.57	1.87	1.36	0.96	0.62	0.33	0.11	0.00
	eigenvalues	3.63	2.97	1.06	0.71	0.42	0.11	0.09	0.01	0.00
	% Variance explained	0.40	0.33	0.12	0.08	0.05	0.01	0.01	0.00	0.00
lineage	aripo	-0.15	-0.50	-0.25	-0.17	0.37	-0.41	-0.27	0.36	0.36
	aripo1	-0.41	-0.24	0.27	-0.04	0.53	0.53	0.00	0.09	-0.36
	guanapo	-0.37	0.38	0.01	-0.25	0.03	0.28	-0.39	-0.32	0.57
	guanapo1	0.23	0.37	-0.08	-0.66	0.44	-0.27	0.11	-0.14	-0.28
	marianne	-0.38	-0.04	-0.49	-0.38	-0.50	0.11	-0.13	0.20	-0.39
	marianne1	-0.47	-0.09	-0.31	0.14	0.11	-0.22	0.62	-0.45	0.08
	quare	0.29	-0.40	0.08	-0.50	-0.19	0.39	0.44	0.00	0.35
	turure	0.32	-0.40	-0.32	0.06	0.07	0.14	-0.39	-0.64	-0.19
	yarra	-0.25	-0.28	0.65	-0.24	-0.29	-0.41	-0.14	-0.29	-0.14

Table 5. Location (LG and bp position) of significantly differentiated SNPs among populations and putative underlying genes. Shaded cells indicate non-genic regions within which SNPs are found.

LG	position	Median XtX	annotated gene	gene description	zebrafish ortholog
LG01	20679153	21.22	ctnna2	catenin (cadherin-associated protein), alpha 2	ctnna2
LG01	21630340	21.84	na		-
LG01	24267902	21.50	na		
LG02	735314	22.89	na		
LG02	3366912	21.21	mid1	midline 1	mid1
LG02	11968486	21.46	na		
LG02	18552459	21.67	LOC103480034	teleost multiple tissue opsin 2b	tmtops2b
LG02	18738097	21.30	LOC103480073	DCN1, defective in cullin neddylation 1, domain containing 2a	dcun1d2a
LG02	23502075	21.57	LOC103481844	potassium voltage-gated channel, subfamily H, member 3	kcnh3
LG02	26822612	21.43	LOC103457726	kalirin-like	kalrnb
LG02	27317080	21.23	na		
LG02	27737287	23.24	tnfsf13b	TNF superfamily member 13b	tnfsf13b
LG03	4026992	21.52	na		
LG03	10136707	22.11	LOC103462047	UPF0469 protein KIAA0907 homolog	uncharacterised
LG04	1388450	21.33	LOC108166264	collagen alpha-1 chain-like	col24a1
LG04	19135875	21.27	LOC103464057	sec1 family domain-containing protein 2	scfd1
LG04	22158698	21.54	LOC103463697	uncharacterised	uncharacterised
LG04	29560803	21.61	elavl4	ELAV like neuron-specific RNA binding protein 4	elavl4
LG04	30040468	21.89	LOC103464223	protein tyrosine phosphatase receptor type Fa	ptprfa
LG04	30061932	21.98	LOC103464223	protein tyrosine phosphatase receptor type Fa	ptprfa
LG04	30108556	21.22	LOC103464223	protein tyrosine phosphatase receptor type Fa	ptprfa
LG04	30110320	21.47	LOC103464223	protein tyrosine phosphatase receptor type Fa	ptprfa
LG04	30492932	21.26	LOC103464192	epidermal growth factor receptor substrate 15-like 1	eps15l1a
LG04	31086053	21.28	pde6d	phosphodiesterase 6D, cGMP-specific, rod, delta	pde6d
LG06	1451327	21.65	dusp6	dual specificity phosphatase 6	dusp6
LG06	7012709	22.19	tmem117	transmembrane protein 117	tmem117
LG06	15480429	21.76	polg	polymerase (DNA directed), gamma	polg
LG06	21928581	21.39	LOC103466341	netrin-4-like	ntn4

LG06	21928809	21.65	LOC103466341	netrin-4-like	ntn4
LG07	1303358	21.33	na		
LG07	9267800	21.91	xpc	xeroderma pigmentosum, complementation group C	xpc
LG07	22765503	21.85	dcaf1	DDB1 and CUL4 associated factor 1	DDB1- and CUL4-associated factor 1-like
LG08	2558818	22.29	LOC103468161	carbonic anhydrase-related protein 10-like	ca10a
LG08	9964866	21.68	clg8h16orf72	linkage group 8 C16orf72 homolog	zgc:66160
LG08	16159265	21.51	lfng	LFNG O-fucosylpeptide 3-beta-N-acetylglucosaminyltransferase	lfng
LG09	5667793	21.49	na		
LG09	7471619	21.61	LOC103469702	protein kinase, AMP-activated, beta 1 non-catalytic subunit, b	prkab1b
LG09	12715576	21.56	LOC103469911	uncharacterised	zgc:152968
LG09	26617339	21.21	LOC103470491	transient receptor potential cation channel, subfamily M, member 3	trpm3
LG09	27956069	21.37	na		
LG09	29207832	21.68	dtx1	deltex 1, E3 ubiquitin ligase	dtx1
LG09	33808366	21.49	prdm6	PR domain containing 6	prdm6
LG10	20059227	21.77	na		
LG10	22172121	21.26	LOC103471396	TSC22 domain family, member 3	tsc22d3
LG10	25748269	22.48	na		
LG11	5785615	21.36	LOC103472064	uncharacterised	uncharacterised
LG11	6043719	21.31	trio	trio Rho guanine nucleotide exchange factor	Trio
LG11	6221092	24.40	rpl14	ribosomal protein L14	rpl14
LG11	11324398	21.83	LOC103472245	calcitonin receptor	calcr
LG11	17282316	21.44	na		
LG11	19054623	21.34	LOC103472636	uncharacterised	uncharacterised
LG11	27311868	21.51	LOC103472993	cyclic GMP-AMP synthase-like	uncharacterised
LG11	28122311	21.85	LOC108166719	uncharacterised	uncharacterised
LG12	3570482	21.77	LOC104373253	macrophage mannose receptor 1-like	rilpl1
LG12	13100673	21.67	LOC103473585	matrix metallopeptidase 17a	mmp17a
LG12	16344388	21.39	na		

LG12	19606315	22.08	na		
LG12	23073848	21.24	LOC103474004	immunoglobulin superfamily, member 9a	igsf9a
LG12	23074083	21.44	LOC103474004	immunoglobulin superfamily, member 9a	igsf9a
LG13	14610669	21.79	tusc5	trafficking regulator of GLUT4 (SLC2A4) 1a	trarg1a
LG14	2734379	22.45	na		
LG14	13371933	21.39	na		
LG14	17753953	21.38	med13	med13	med13a
LG15	6448226	21.22	na		
LG15	7538997	22.53	na		
LG16	12769623	21.42	pianp	PILR alpha associated neural protein	pianp
LG17	963224	21.33	LOC103478874	TOX high mobility group box family member 4 a	tox4a
LG17	4792866	21.46	lrp8	low density lipoprotein receptor-related protein 8, apolipoprotein e receptor	lrp8
LG17	15468027	21.77	na		
LG17	30749000	22.27	slc39a6	solute carrier family 39 member 6	slc39a6
LG18	1955592	21.43	LOC103480181	neurexin-2-beta-like	uncharacterised
LG18	2195221	22.31	na		
LG19	1718516	21.38	rab11fip3	RAB11 family interacting protein 3 (class II)	rab11fip3
LG19	7450869	21.63	LOC103481309	uncharacterised	uncharacterised
LG19	14860722	21.29	ttyh2	tweety family member 2	ttyh2
LG19	21916746	21.34	LOC108167282	uncharacterised	uncharacterised
LG20	12634650	22.26	LOC103482504	uncharacterised	uncharacterised
LG20	12638410	21.91	LOC103482504	uncharacterised	uncharacterised
LG20	23266788	21.93	ptprn2	protein tyrosine phosphatase receptor type N2	ptprn2
LG21	1839279	21.90	LOC103457165	AT rich interactive domain 1B (SWI1-like)	arid1b
LG22	10792343	21.27	na		
LG22	13499891	21.28	kiz	kizuna centrosomal protein	kiz
LG23	1038549	21.87	LOC103459116	protein FAM180A-like	FAM180A
LG23	1038658	21.34	LOC103459116	protein FAM180A-like	FAM180A
LG23	10260495	22.01	na		

Figure Legends:

Figure 1. Example of photography setup using calibrated photography using visible and UV spectrum (grayscale). Black and white blocks are 5% and 95% reflectance standards, respectively.

Figure 2. Distribution of population mean trait values (prior to conversion to SDU) by predation regime and population under guppy and pike cichlid vision models for (a) colour saturation ($sat_{\Delta S}$), (b) luminance ($lum_{\Delta S}$), (c) chromaticity ($chrom_{\Delta S}$), (d) coefficient of variation in chromaticity ($chrom_{\Delta S}$). Lines link populations of differing regime within rivers. Also shown are the overall trait means by predation regime (red circle) with standard error. Asterisk (*) denotes significant difference in overall mean between regimes. Note that Paria (light blue square) does not have a corresponding high predation population.

Figure 3. Neighbour joining trees of populations based on estimated phenotypic distance matrices in n-dimensional trait space. Tree shown are determined using (a) all eight colour measures, (b) the four traits derived from the guppy-and (c) the four traits derived from the cichlid-vision model. Red and blue labels denote high and low predation *regime* populations, respectively.

Figure 4. Between-population distance estimates based on guppy (x-axis) and cichlid (y-axis) vision models. Each point denotes a single pairwise population comparison. Red points denote cross-regime distances between a high and a low predation site and blue points denote pairwise distances within predation regimes (dark blue for high, light blue for low), Ellipses illustrate approximate 95% confidence limits of the distributions and the 1:1 line is also shown.

Figure 5. Neighbor joining tree based on whole-genome population F_{ST} distance, clustering by rivers, then drainages, consistent with the independent evolution of each replicate. Branch length represents Fst. Populations: AH = Aripo High; AL = Aripo Low; AL2 = Aripo Low 2; GH = Guanapo High; MH = Marianne High; ML = Marianne Low; PML = Petite Marianne; PL = Paria; QH = Quare High; QL = Quare Low; YH = Yarra High; YL = Yarra Low. Blue denotes Low predation regime, whereas Red High.

Figure 6. Manhattan plot of genome-wide differentiation among 12 male populations of guppies. The red dotted line and points indicate the 0.01% (21.2 *XtX*) threshold and significantly differentiated SNPs, respectively. Red dots denote significantly differentiated SNPs. Labels above dots denote putative candidate genes implicated cell morphogenesis linked to color patterns.

Figure S1. Illustration of the covariance matrix **Ω** among 12 populations estimated from BayPass core model using ca. 100,000 SNPs.

Figure S2. Eigen decomposition of C matrices for (a) guppy- (b) cichlid- (c) guppy and cichlid-perceived color patterns, demonstrating general support for the null hypothesis of independent change in color patterns. Red dots and line indicate observed values from diagonalization of the estimated matrix C. Per De Lisle and Bolnick (2020), green and boxplots represent the expected distribution of eigenvalues under a null hypothesis of a random direction of evolutionary change across lineages, calculated from sampling the corresponding Wishart distribution or an simulated distribution by placing random vectors in a trait space (1000 simulations)

Fig.1

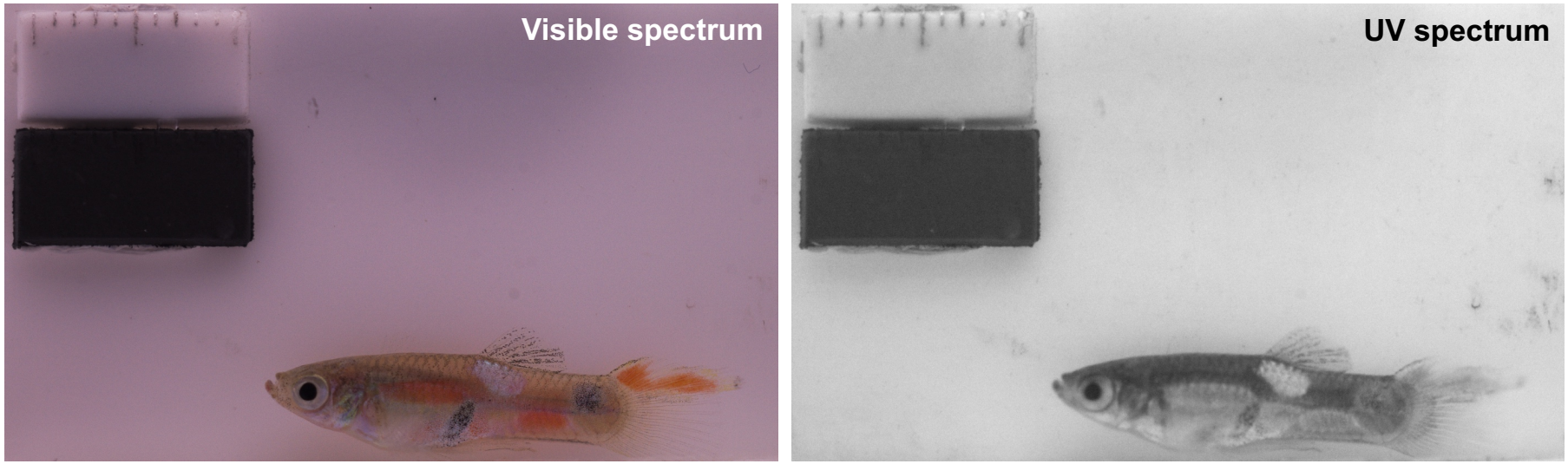

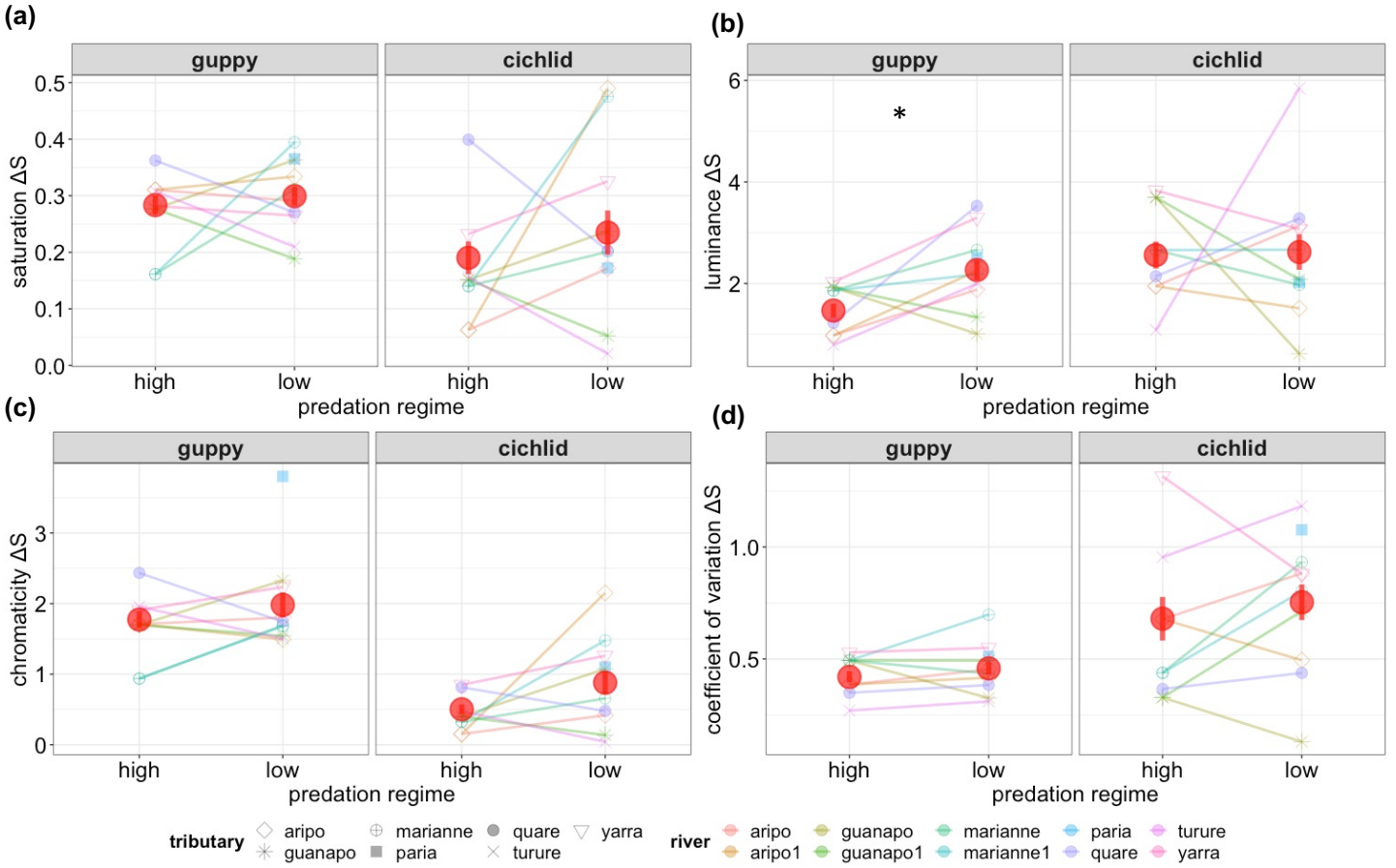
(a)
guppy
cichlid
saturation ΔS
0.5
0.4
0.3
0.2
0.1
0.0
high
low
high
low
predation regime
(b)
guppy
cichlid
luminance ΔS
6
4
2
*
high
low
high
low
predation regime
(c)
guppy
cichlid
chromaticity ΔS
3
2
1
0
high
low
high
low
predation regime
(d)
guppy
cichlid
coefficient of variation ΔS
1.0
0.5
high
low
high
low
predation regime
tributary
aripo
guanapo
marianne
paria
quare
turure
yarra
river
aripo
aripo1
guanapo
guanapo1
marianne
marianne1
paria
quare
turure
yarra

Fig. 3

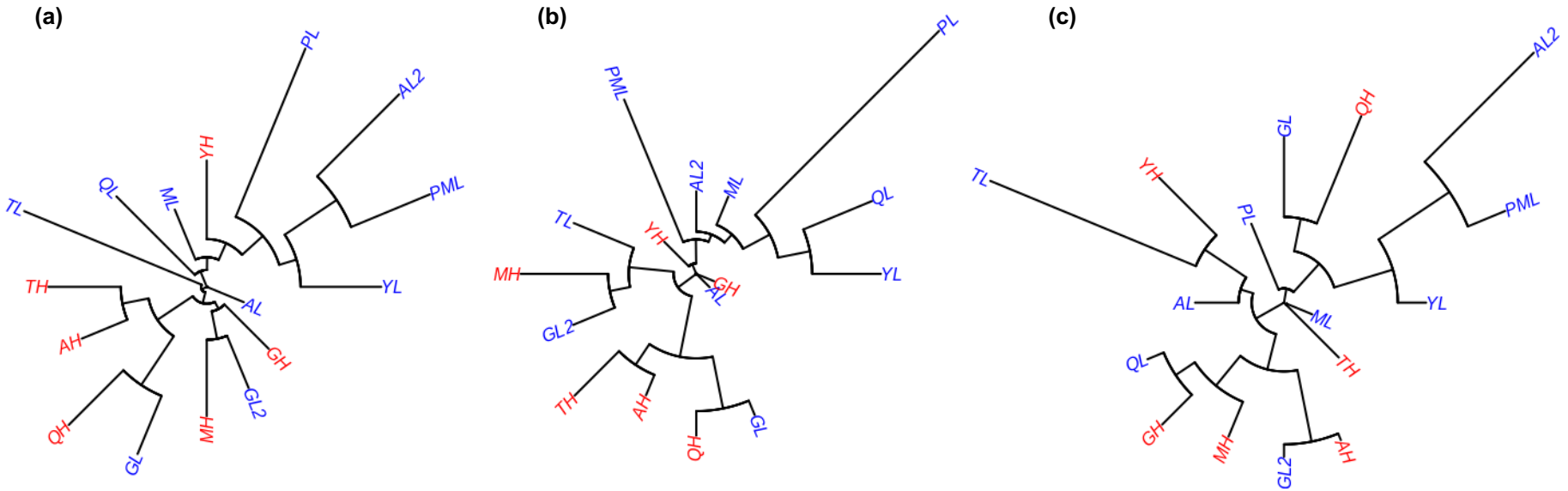
(a)
PL
AL2
PML
YH
QL
ML
TL
YL
TH
AL
AH
GH
QH
GL2
GL
MH
(b)
PL
PML
AL2
ML
QL
TL
YH
YL
MH
GH
AL
GL2
TH
AH
GL
QH
(c)
AL2
GL
QH
YH
PML
PL
TL
YL
AL
ML
QL
TH
GH
MH
GL2
AH

Fig. 4

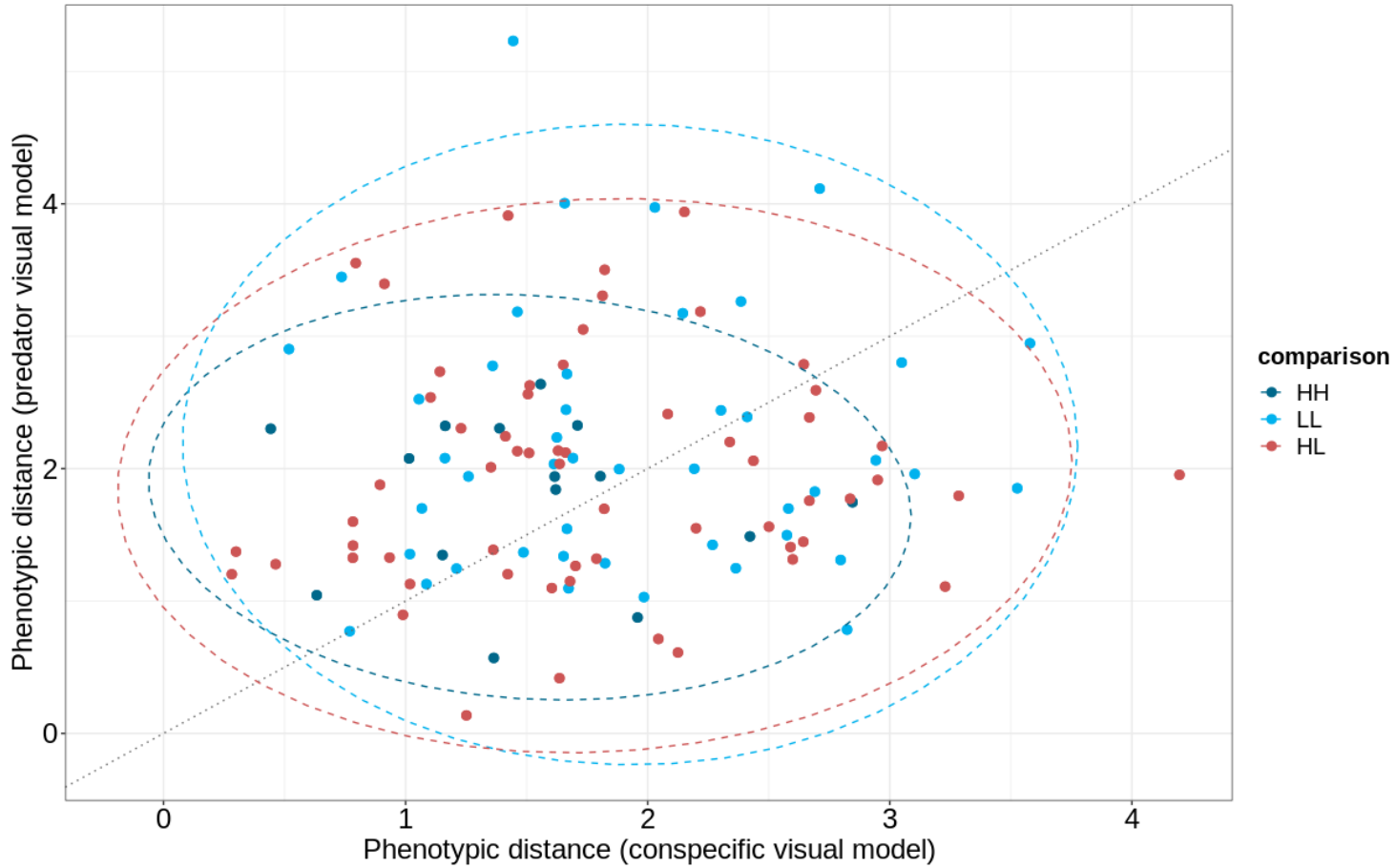
Phenotypic distance (predator visual model)
0
2
4
0
1
2
3
4
Phenotypic distance (conspecific visual model)
comparison
HH
LL
HL

Fig. 5

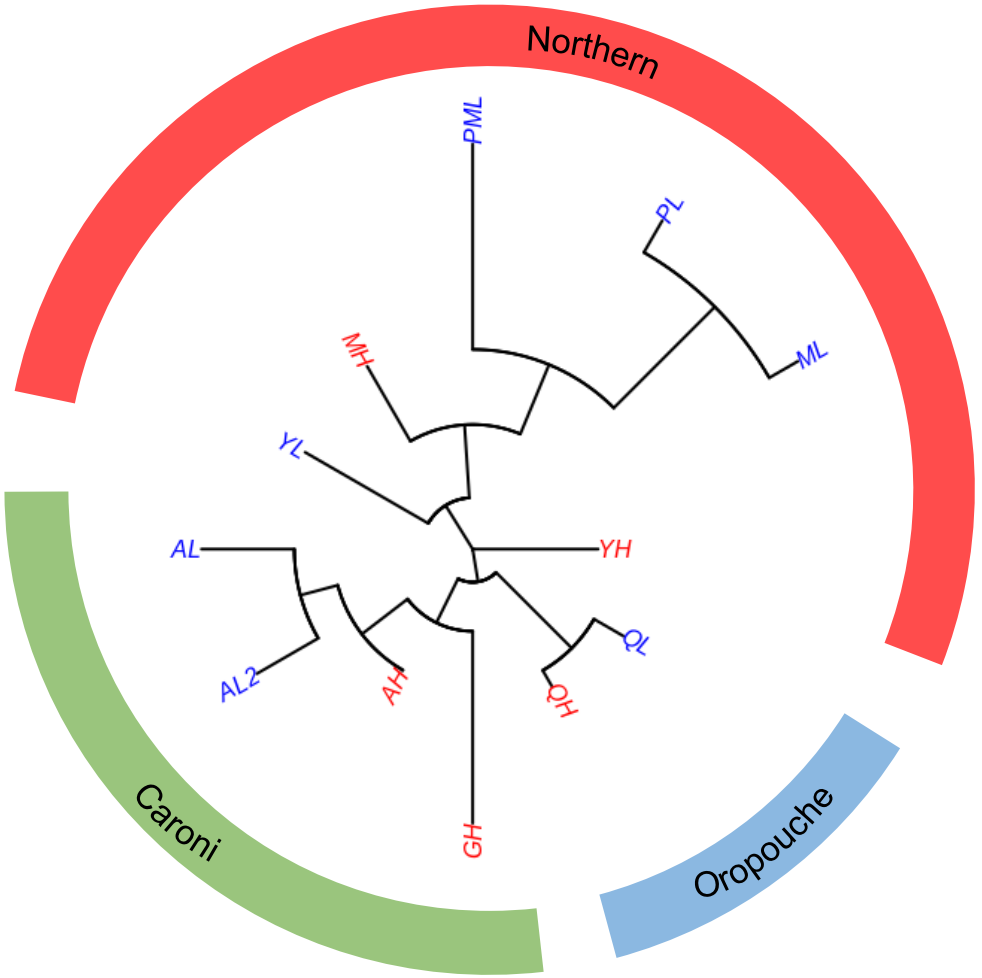

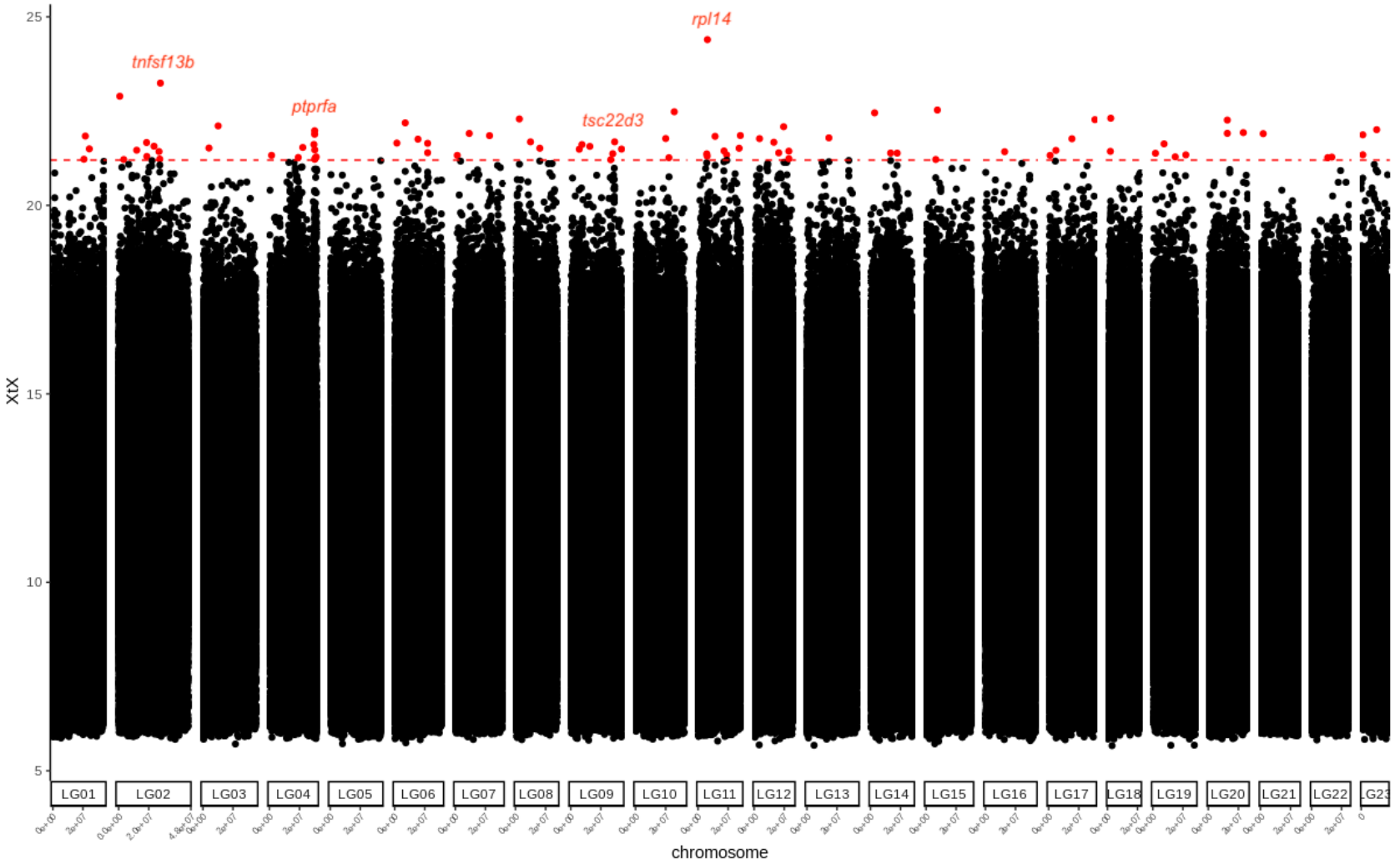
tnfsf13b
ptprfa
tsc22d3
rpl14
XtX
chromosome
LG01
LG02
LG03
LG04
LG05
LG06
LG07
LG08
LG09
LG10
LG11
LG12
LG13
LG14
LG15
LG16
LG17
LG18
LG19
LG20
LG21
LG22
LG23

Fig. 6

Fig. S1

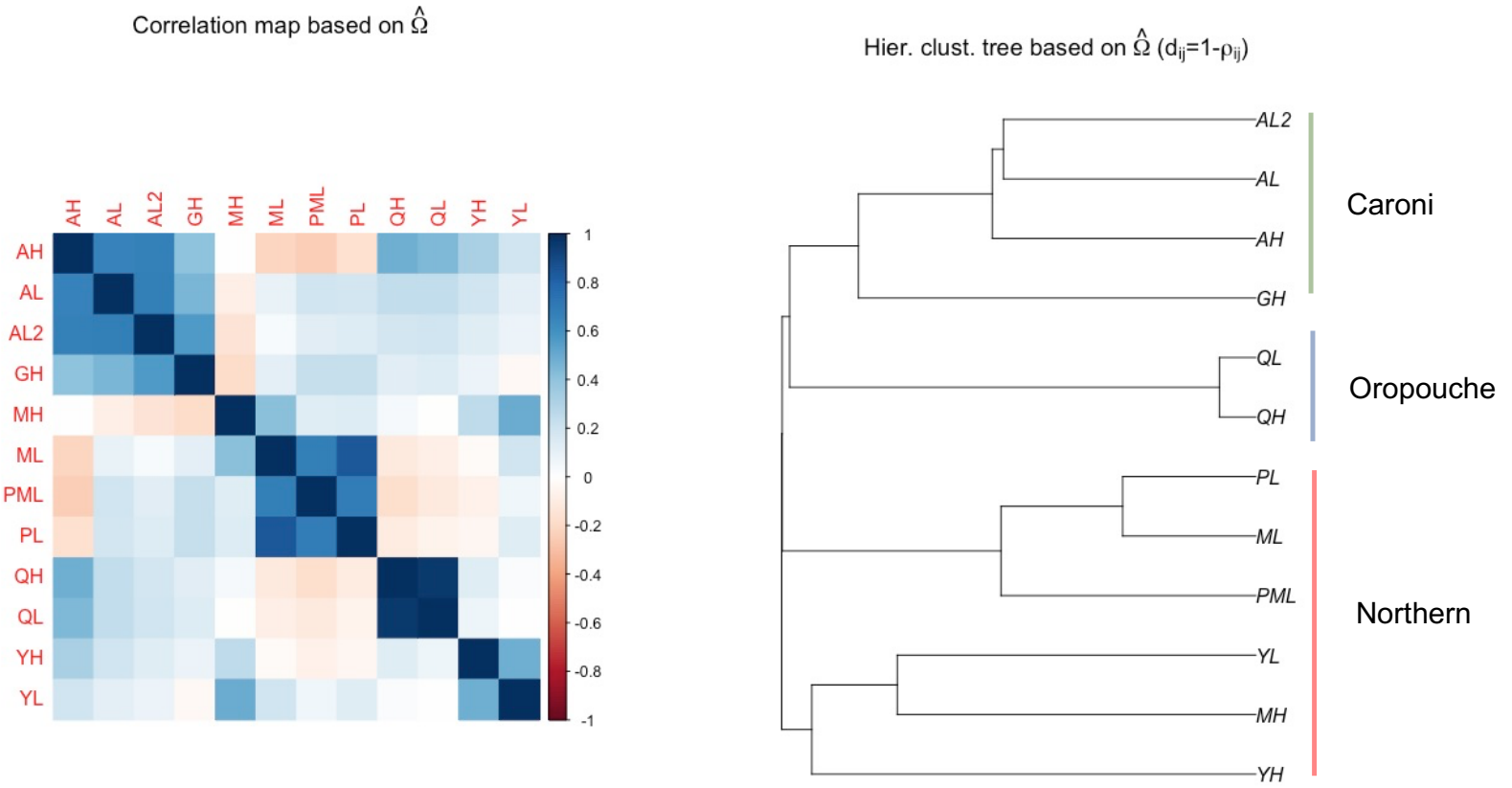
Correlation map based on $\hat{\Omega}$
AH
AL
AL2
GH
MH
ML
PML
PL
QH
QL
YH
YL
1
0.8
0.6
0.4
0.2
0
-0.2
-0.4
-0.6
-0.8
-1
Hier. clust. tree based on $\hat{\Omega}$ (d_{ij}=1-ρ_{ij})
AL2
AL
AH
GH
QL
QH
PL
ML
PML
YL
MH
YH
Caroni
Oropouche
Northern

Fig. S2

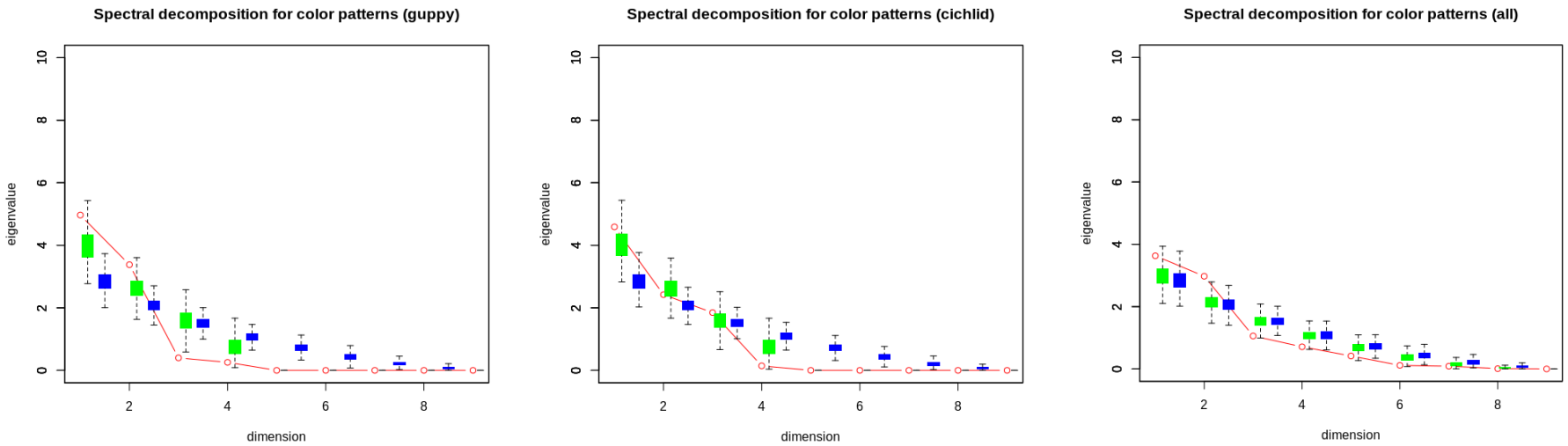
Spectral decomposition for color patterns (guppy)
eigenvalue
dimension
0
2
4
6
8
10
Spectral decomposition for color patterns (cichlid)
eigenvalue
dimension
Spectral decomposition for color patterns (all)
eigenvalue
dimension